AD-A184 456 LASER INDUCED FLUORESCENT STUDY OF RELATIVISTIC ELECTRON BEAMS(U) HY-TECH RESEARCH CORP RADFORD VA E J YADLOWSKY ET AL JUN 87 AFWL-TR-85-140 1/1

UNCLASSIFIED F29601-83-C-0024 F/G 20/7 NL

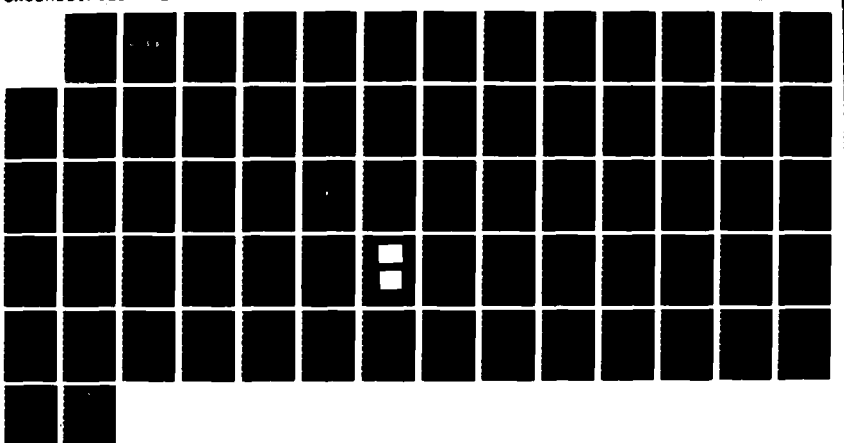

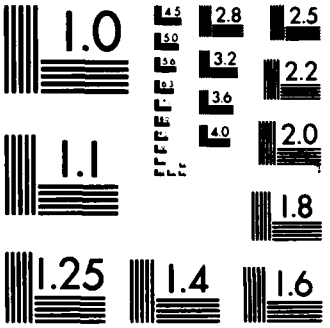

AFWL-TR-
85-140

(2)

LASER INDUCED FLUORESCENT STUDY OF RELATIVISTIC ELECTRON BEAMS

Edward J. Yadlowsky
Robert C. Hazelton

HY-TECH Research Corporation
Radford, VA 24143

June 1987

Final Report

Approved for public release; distribution unlimited.

AIR FORCE WEAPONS LABORATORY
Air Force Systems Command
Kirtland Air Force Base, NM 87117-6008

This final report was prepared by HY-TECH Research Corporation, Radford, Virginia, under Contract F29601-83-C-0024, Job Order 2301Y101 with the Air Force Weapons Laboratory, Kirtland Air Force Base, New Mexico. Mr Ray Lemke (AWPB) was the Laboratory Project Officer-in-Charge.

When Government drawings, specifications, or other data are used for any purpose other than in connection with a definitely Government-related procurement, the United States Government incurs no responsibility or any obligation whatsoever. The fact that the Government may have formulated or in any way supplied the said drawings, specifications, or other data, is not to be regarded by implication, or otherwise in any manner construed, as licensing the holder, or any other person or corporation; or as conveying any rights or permission to manufacture, use, or sell any patented invention that may in any way be related thereto.

This report has been authored by a contractor of the United States Government. Accordingly, the United States Government retains a nonexclusive, royalty-free license to publish or reproduce the material contained herein, or allow others to do so, for the United States Government purposes.

This report has been reviewed by the Public Affairs Office and is releasable to the National Technical Information Services (NTIS). At NTIS, it will be available to the general public, including foreign nations.

If your address has changed, if you wish to be removed from our mailing list, or if your organization no longer employs the addressee, please notify AFWL/AWPB, Kirtland AFB, NM 87117-6008 to help us maintain a current mailing list.

This technical report has been reviewed and is approved for publication.

Ray Lemke

RAY LEMKE
Project Officer

FOR THE COMMANDER

Bruce R. Anderson

BRUCE R. ANDERSON
Major, USAF
Chief, Beam Physics Branch

William L. Baker

WILLIAM L. BAKER, PhD
Chief, Advanced Technology Division

DO NOT RETURN COPIES OF THIS REPORT UNLESS CONTRACTUAL OBLIGATIONS OR NOTICE ON A SPECIFIC DOCUMENT REQUIRES THAT IT BE RETURNED.

UNCLASSIFIED

SECURITY CLASSIFICATION OF THIS PAGE

AD-A184 256

REPORT DOCUMENTATION PAGE

1a. REPORT SECURITY CLASSIFICATION UNCLASSIFIED	1b. RESTRICTIVE MARKINGS
2a. SECURITY CLASSIFICATION AUTHORITY	3. DISTRIBUTION/AVAILABILITY OF REPORT Approved for public release; distribution unlimited.
2b. DECLASSIFICATION DOWNGRADING SCHEDULE	
4. PERFORMING ORGANIZATION REPORT NUMBER(S)	5. MONITORING ORGANIZATION REPORT NUMBER(S) AFWL-TR-85-140
6a. NAME OF PERFORMING ORGANIZATION HY-TECH Research Corporation 6b. OFFICE SYMBOL (If applicable)	7a. NAME OF MONITORING ORGANIZATION Air Force Weapons Laboratory
6c. ADDRESS (City, State and ZIP Code) P.O. Box 3422 Radford, VA 24143	7b. ADDRESS (City, State and ZIP Code) Kirtland Air Force Base, NM 87117-6008
8a. NAME OF FUNDING/SPONSORING ORGANIZATION 8b. OFFICE SYMBOL (If applicable)	9. PROCUREMENT INSTRUMENT IDENTIFICATION NUMBER F29601-83-C-0024
8c. ADDRESS (City, State and ZIP Code)	10. SOURCE OF FUNDING NOS PROGRAM ELEMENT NO: 61102F; PROJECT NO: 2301; TASK NO: Y1; WORK UNIT NO: 01
11. TITLE (Include Security Classification) LASER INDUCED FLUORESCENT STUDY OF RELATIVISTIC ELECTRON BEAMS	
12. PERSONAL AUTHOR(S) Yadlowsky, Edward J., and Hazelton, Robert C.	
13a. TYPE OF REPORT Final 13b. TIME COVERED FROM 28Apr83 TO 31Jan86	14. DATE OF REPORT (Yr., Mo., Day) 1987 June 15. PAGE COUNT 72
16. SUPPLEMENTARY NOTATION	

17. COSATI CODES		
FIELD	GROUP	SUB GR
20	07	

18. SUBJECT TERMS (Continue on reverse if necessary and identify by block number)
Relativistic electron beam
Laser-induced fluorescence
Electron beam propagation
Zeeman effect
Stark effect

19. ABSTRACT (Continue on reverse if necessary and identify by block number)

The magnetic fields associated with a relativistic electron beam propagating in a gas provide information about the net current distribution in the beam and the stability of the beam with respect to hose, hollowing, and flute instabilities. In principle, these magnetic fields can be measured using Faraday rotation techniques, or by measuring the Zeeman splitting of atomic/ionic transitions using emission spectroscopy. Both of these techniques lack longitudinal and spatial resolution since they integrate the effect of the magnetic field along the line-of-sight of the instrument. This work investigates the measurement of magnetic field contours by optically pumping atoms/ions with a narrow band dye laser tuned to a Zeeman shifted electronic transition, and recording the fluorescence radiation emitted perpendicular to the excitation laser. This technique has important advantages over conventional optical techniques because the dye laser is the frequency selective element and the magnetic field measurement is reduced to an intensity measurement with the spatial resolution determined by the irradiated volume viewed by the collection optics. (over)

20. DISTRIBUTION/AVAILABILITY OF ABSTRACT UNCLASSIFIED/UNLIMITED X SAME AS RPT ☐ DTIC USERS ☐	21. ABSTRACT SECURITY CLASSIFICATION UNCLASSIFIED
22a. NAME OF RESPONSIBLE INDIVIDUAL Ray Lemke	22b. TELEPHONE NUMBER (Include Area Code) (505) 844-0121 22c. OFFICE SYMBOL AWPB

DD FORM 1473, 83 APR EDITION OF 1 JAN 73 IS OBSOLETE

UNCLASSIFIED

SECURITY CLASSIFICATION OF THIS PAGE

19. ABSTRACT (Continued)

The studies were carried out in a high current ~~(0.9 - 4.0 kA)~~ discharge operated in neon and neon/nitrogen mixtures at pressures of 0.1 to 2 kPa. A grazing incidence flash lamp pumped dye laser having a band width of 0.004 to 0.009-nm was used to fluoresce the 585.25-nm transition in neutral neon. The frequency spectrum of the radiation was recorded with a photomultiplier by scanning the laser frequency. The measurements reveal an LIF spectrum which is double-humped under certain conditions. The overall width of the spectrum is consistent with the Stark broadened line width anticipated for the plasma condition, and the minimum at the line center cannot be attributed to self absorption in the plasma.

The results could be interpreted as a Zeeman broadened spectrum if the bulk of the current is assumed to flow in a channel having a diameter approximately 1/4 the size of the luminous channel diameter.

Although additional studies are required to determine the origin of the double-humped feature, the Zeeman split interpretation suggests that this diagnostic technique may be applicable under the conditions that were investigated.

ACKNOWLEDGMENTS

The authors would like to thank Mr R.T. Graham, Hi-Tech Research Corporation, for his help in carrying out the experiments, and Ms R. Yadlowsky for typing the manuscript.

CONTENTS

I. INTRODUCTION

BACKGROUND

A knowledge of the electric and magnetic fields associated with a relativistic electron beam (REB) propagating in a gas is of great interest because these fields influence the stability of the beam. Electron heating and ionization by electric fields in the beamhead determine the conductivity profile and return current profile. The magnetic fields in the pinched portion of the beam are directly related to the interaction of the beam current with the return current and are a measure of the hollowing, hose and flute instabilities which can catastrophically affect the beam propagation. In principle these fields can be measured by conventional emission spectroscopy by first spatially resolving the area studied to localize the sampled volume and then frequency resolving the emitted radiation to determine the Stark or Zeeman shift. The field value can be inferred from the measured shift. The technique requires the frequency resolved spectrum to be temporally resolved to study the time evolution of the field strength. The technique is further complicated by the fact that all the atoms in the plasma volume subtended by the collection optics contribute to the detected signal. The resulting lack of longitudinal spatial resolution results in apparent broadening of the observed radiation spectrum due to spatially varying field strengths.

The research program described by this report is concerned with developing a laser-induced fluorescence (LIF) technique for measuring the electric and magnetic field strengths in an REB propagation study. The LIF technique is an active spectroscopic diagnostic that employes a dye laser tuned to an electronic transition frequency of a neutral or ionic specie (the target) to resonantly excite the target to a higher energy state. The fluorescence radiation viewed perpendicular to the pump laser is recorded using a narrow band filter to discriminate against background radiation. If the line width of the exciting laser is larger than the absorption line width of the target specie, then the spatial distribution of the LIF radiation is a measure of the number density of targets in the excited state probed. This has been used to measure neutral densities in Tokomaks (Ref. 1) and ion concentrations in radio frequency (RF) sheaths (Ref. 2). If the line width of the laser is less than the absorption width, only those atoms

in resonance with the laser will absorb and radiate. If the broadening is due to thermal motion or bulk streaming, the frequency spectrum of LIF radiation is a measure of the ion velocity distribution. If the broadening is due to electric or magnetic fields, then the frequency spectrum, spatially resolved is a measure of the local field strength. Researchers are currently trying to develop the LIF technique to measure magnetic fields in fusion devices (Refs. 3,4), and electric fields and magnetic fields in ion diodes (Ref. 5).

The LIF technique offers three important advantages over emission spectroscopy. First, the use of resonance radiation to optically pump selected transitions results in improved signal-to-noise (SNR) characteristics and greater sensitivity. Second, the lifetime of the upper state is determined by the stimulated emission rate which can be made extremely short by using intense lasers. In this way the time resolution is determined by the response time of the detector circuits, not the radiative and collisional depopulation rates as in emission spectroscopy. Finally, the dye laser is the frequency selective element in the system. Interference filters at the detectors are sufficient to distinguish the fluorescence radiation, and spatial distribution measurements are reduced to intensity distribution measurements without Abel inversion.

An important feature of the LIF technique (which the diagnostics development program described herein seeks to exploit) is the recording of magnetic field contours in a rapidly varying pulsed environment. This can be accomplished by tuning the laser to a Zeeman shifted frequency corresponding to magnetic field H_1. If the narrow diameter laser beam is directed radially through the REB channel, then only those atoms at the radial positions corresponding to the magnetic field strength H_1 will fluoresce. If this radiation is focused onto the input slit of a streak camera, then the temporal variation of the H_1 magnetic field contour is recorded.

OVERVIEW OF RESEARCH PROGRAM

The research effort consists of a proof-of-principle phase (Phase I) concerned with establishing the applicability of the LIF technique for REB propagation studies and an investigative phase (Option I) concerned with making measurement on a REB system. This report will describe the Phase I

work done to determine if frequency shifts in spectral lines of atoms and ions due to magnetic and electric fields can be detected and resolved under conditions approximating those encountered in REB systems. The work was carried out in a high current discharge to simulate the pinched portion of the propagating beam. In the original proposal, neon would be added as a tracer to the background gas and the Zeeman shift of the 585.25-nm NeI transition would be studied. This line was chosen because of its simple Zeeman spectrum and relatively modest Stark broadening. During the course of the work, the effort was expanded to consider the 566.66-nm line of singly ionized atomic nitrogen. This latter candidate was added because this was an atomic ion line that should occur in an REB propagation experiment in air that is reasonably isolated, intense, and accessible within the wavelength selection limitation of the laser optics currently in-house. Ionic lines are of interest in high pressure propagation experiments because the Stark broadening of these lines is less than for neutral lines (approximately an order of magnitude in some cases) (Refs. 6,7), and is expected to be less for broadening by neutrals as well (Ref. 8).

In the course of this study, high current discharges (0.5 - 40 kA) were generated using a capacitive discharge system for backfill pressures in the range of 10-Pa to 20-kPa in argon, neon, nitrogen and neon-nitrogen mixtures. The discharge was characterized using Langmuir probes, emission spectroscopy, and open shutter photographs. Laser-induced fluorescence spectra and absorption spectra were obtained for the 585.25 NeI line using a pulsed dye laser to scan the line profile. Broadening of the LIF spectral line and double humped features in the line profile indicate that Zeeman shifting of the line might have been observed. Magnetic field contours were not recorded in the present work because of limitation in the streak camera. Electron temperatures inferred from the LIF measurement are in between the values obtained with the Languir probe and the values inferred from absorption or line intensity ratio measurements. The unsuccessful attempts to measure LIF on the N II 566.67-nm line are not explained at this time. Theoretical analysis of the feasibility of using the LIF technique to measure magnetic field contours has been carried out for an REB with a net beam current of 20-kA propagating in air at pressures of 8.4 and 84 kPa. The results indicate that the 585.25 NeI line can be used to probe the magnetic

field for radial positions greater than 0.9 cm at 8.4 kPa, whereas the 566.66-nm N II line can be used to probe down to 0.25 cm at both pressures.

The next section presents a brief description of the theory of LIF spectroscopy and an analysis of the applicability of the contour approach to measuring magnetic fields in REB propagation experiments. This is followed by the section which discusses the high current discharge used as spectroscopic source for this work. A description of the experimental setup for the LIF measurements, the calibration procedure and the LIF studies on the 585.25-nm line of NeI are presented in Section IV. Section V discusses the results and suggests topics for future work.

II. THEORY OF LASER-INDUCED FLUORESCENCE AND APPLICABILITY TO REB PROPAGATION STUDIES

The minimum magnetic field strength, and the signal level that can be observed under REB propagation conditions, can be estimated from the anticipated Zeeman splitting of the lines, the sensitivity of LIF processes, and the estimated background fluorescence level. These quantities are calculated next.

ZEEMAN SPLITTING OF ATOMIC TRANSITIONS

The energy levels of an atomic system are split relative to the zero field case by an amount

$$\Delta E = g' \mu_B H m_J \tag{1}$$

where μ_B is the Bohr magneton, H the field strength in gauss, m_J the Z component of the total angular momentum, and g' the Lande' g factor. This is shown in Figs. 1 - 3 for the energy levels of the 535.25 transition in NeI and the 566.66, 593.18 and 568.62-nm transitions in N II. The Zeeman shift in the wavelength of the spectral line is given by the expression

$$\Delta \lambda = \lambda^2 (0.0046) P H \tag{2}$$

where P is the difference in the products of the Lande'g' factors and Z components of the angular momentum

$$P = (m_k g'_k - m_i g'_i) \tag{3}$$

The wavelength shifts for the various components are given in Table 1 and the relative splitting is shown in Figs. 1 - 3. These lines were chosen because they are reasonably isolated from other interfering lines to facilitate discrimination with interference filters, are reasonably intense for good sensitivity, and have a reasonably simple Zeeman spectrum, since the total J of the energy levels involved is small (1 - 2). The spectra can be further simplified by a judicious choice of polarization of the

excitation laser and detection system. The polarization of the π radiation ($\Delta m_J = 0$) is parallel to the magnetic field direction when viewed perpendicular to the field. The π transition is not observed along the field lines. The polarization of the σ components ($\Delta m_J = \pm 1$) are linearly polarized perpendicular to the magnetic field when viewed transverse to the field. The lower frequency component is left circularly polarized when viewed along the magnetic field direction, whereas the up shifted component is right circularly polarized. P. Weber is utilizing these differences in the π and σ components to study the direction of the magnetic fields in a toroidal confinement device (Ref. 3).

TABLE 1. ZEEMAN SHIFTS (in nm/kg) AND STARK WIDTHS (in nm/cm^3) OF CANDIDATE NII AND NeI LINES

p	λ	$\Delta\lambda_H$	$\Delta\lambda$ (STARK)
1.5 1.167 0.834 0.333	593.18 N II	0.0024 nm/kG 0.00186 0.0013 0.0005	0.00197 $N_e x10^{-16}$
1.5 1.167 0.834 0.333	566.66 N II	0.0022 0.00172 0.00123 0.0005	0.00163 $N_e x10^{-16}$
1.5 0.5 1	568.62 N II	0.0022 0.0007 0.0015	0.00163 $N_e x10^{-16}$
034	585.2 NeI	0.00165	0.0069 $N_e x10^{-16}$

Ne I 5852.5

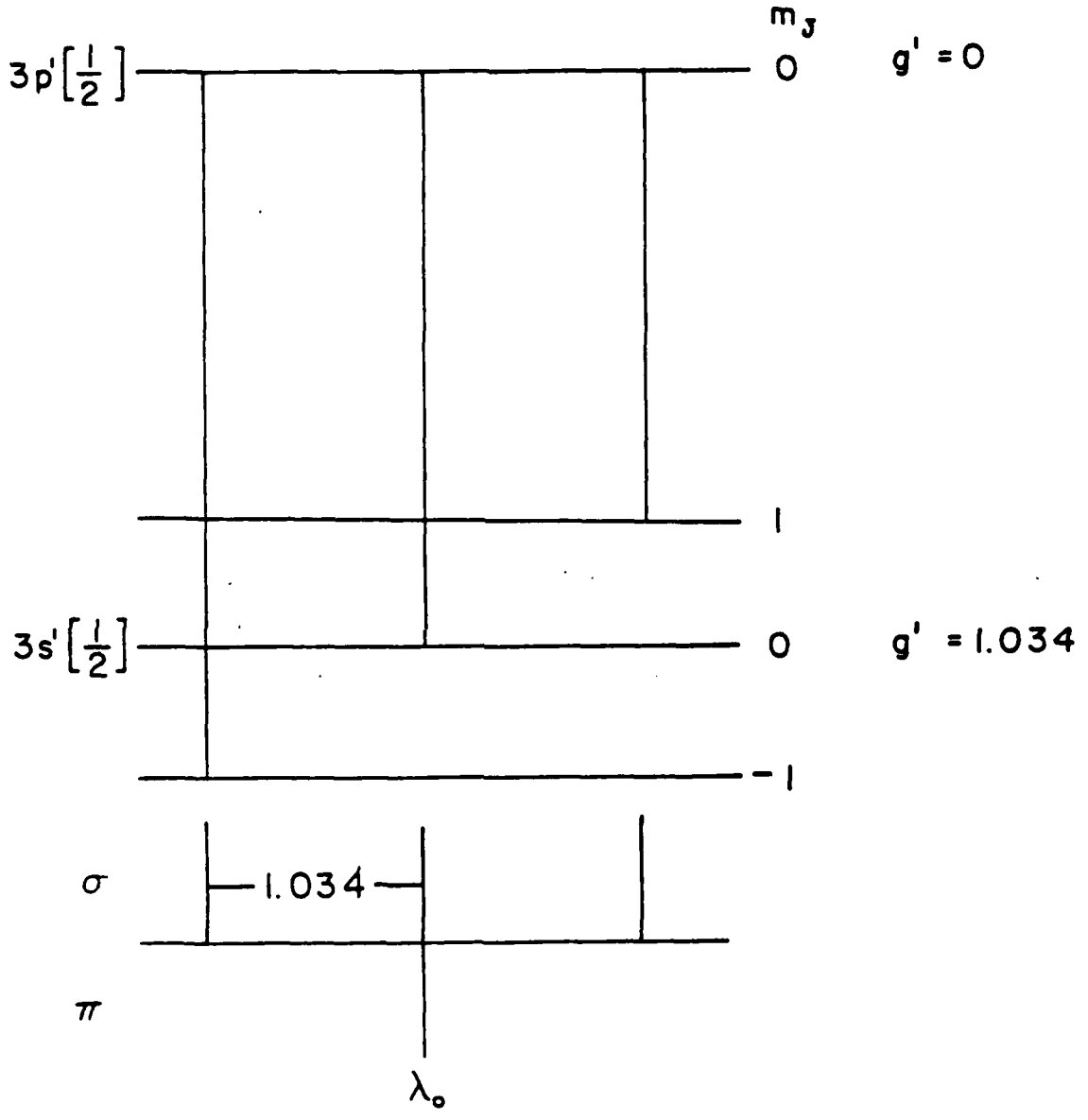

Figure 1. Zeeman splitting of the 585.25-nm transition in neutral neon in terms of the P factor defined in Eq. 3. (The sigma transitions are shown above the reference line and the pi transition is below.)

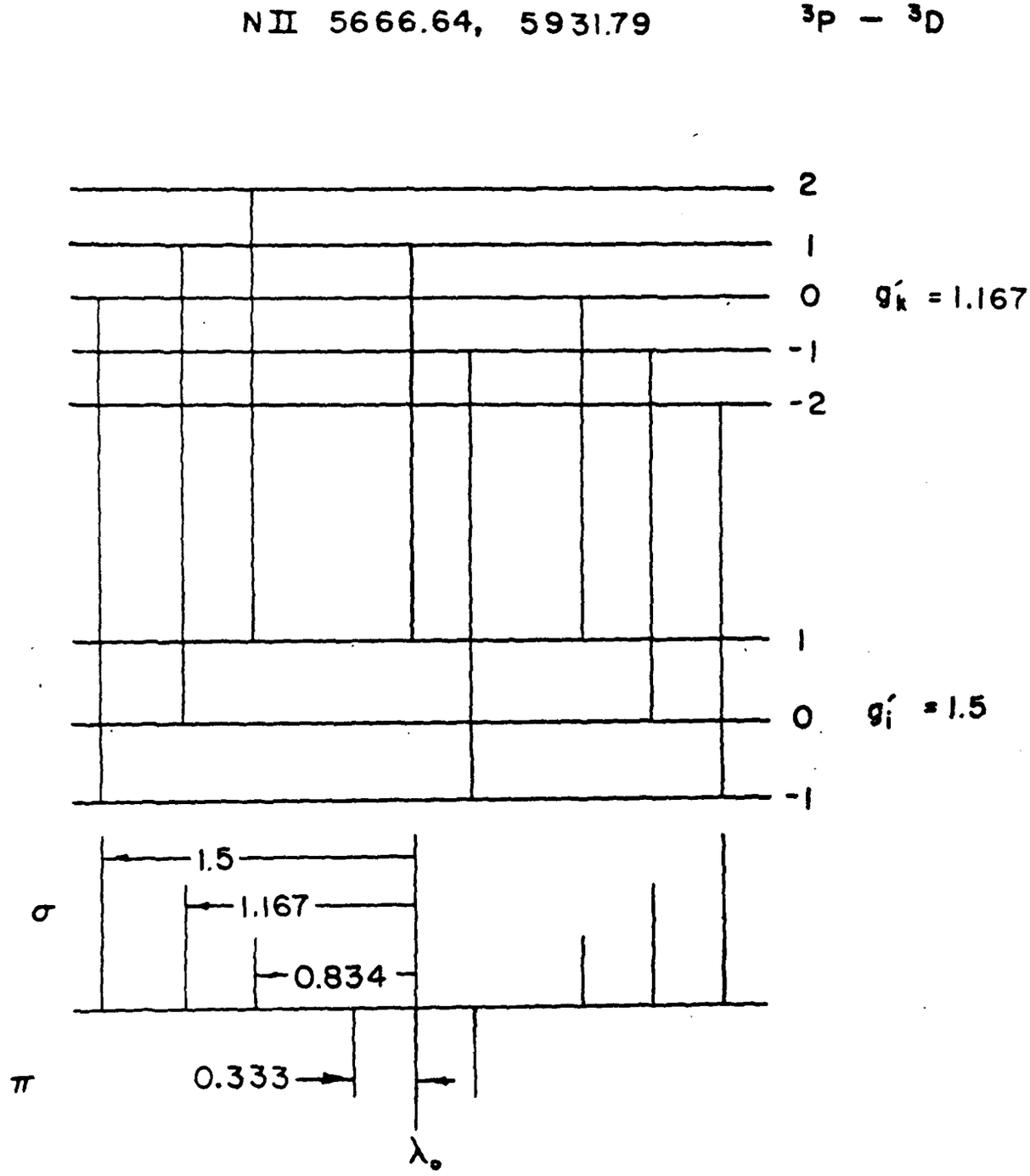

Figure 2. Zeeman splitting of two transitions in ionized atomic nitrogen in terms of the P factor defined in Eq. 2. (The sigma transitions are shown above the reference line and the pi transitions are below.)

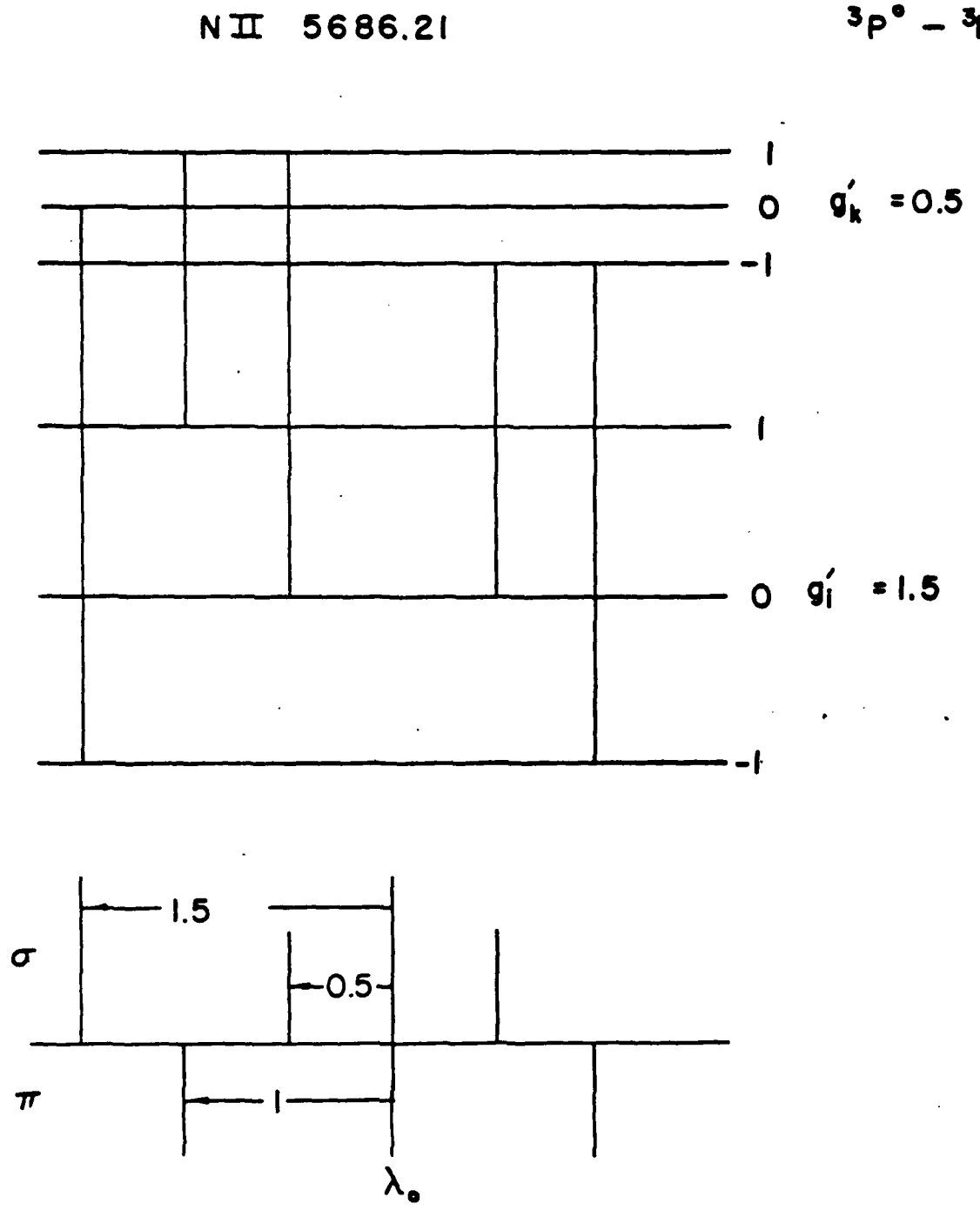

Figure 3. Zeeman splitting of the 568.61-nm line in ionized atomic nitrogen in terms of the P factor defined in Eq. 3. (The sigma transitions are shown above the reference line and the pi transitions are below.)

The information about the magnetic field that can be inferred from an LIF measurement depends on the system geometry and recording procedure. A laser tuned to a Zeeman shifted frequency corresponding to a magnetic field H_1 will cause all the atoms situated in that field to fluoresce. The fluorescent radiation and the background emission are imaged onto the focal plane of the detector system (Fig. 4). If a photomultiplier is used without any limiting apertures, the entire interaction region along the beam is viewed. In this case there is no spatial resolution, and the LIF spectrum obtained by sweeping the laser frequency is an integral of the Zeeman shifts occurring in regions with different magnetic field strengths weighted by the local plasma density. If the photomultiplier is limited by an aperture, then the photomultiplier is viewing a limited region in the plasma. Now, the LIF spectrum is a measure of the magnetic field in the plasma volume determined by the intersection of the laser beam (i.e., the image of the aperture onto the laser beam) and detector optics. This procedure provides spatial resolution but requires a scan over the Zeeman shifted frequency spectrum. If a framing camera is used to record the fluorescent radiation, then the image of the fluorescent radiation is two points on the H_1 magnetic field contour, as shown in Fig. 4. If the field is time dependent, then a streak image of the interaction region produces a time-dependent magnetic field contour, yielding spatial, temporal, and field strength information. In a simple Zeeman spectrum like the NeI 585.25 doublet, only one magnetic field strength corresponds to a given laser frequency, and the resulting fluorescence intensity produces an $H = H_1$ contour. However, in a more complex spectrum like the 566.66-nm line of N II, a given laser frequency corresponds to a number of magnetic field strengths associated with different multiplets of the transition (see Fig. 5). In this case a given laser frequency resonant with targets in four different magnetic field strengths corresponding to the four multiplets in the transition. The resulting fluorescence intensity distribution will produce contours corresponding to these four field strengths if they occur in the volume probed. If the intensities of the four multiplets is sufficient to record, and if the line width is sufficiently narrow to spatially resolve these contours, the measurement technique suggests the possiblity of recording the spatial profile of the magnetic field, temporally resolved. As pointed out above,

polarizers on the laser or detection optics can reduce the complexity of the spectrum by eliminating the π or σ components. Note that the multiplet components do not have equal oscillator strengths and consequently their intensities will be different.

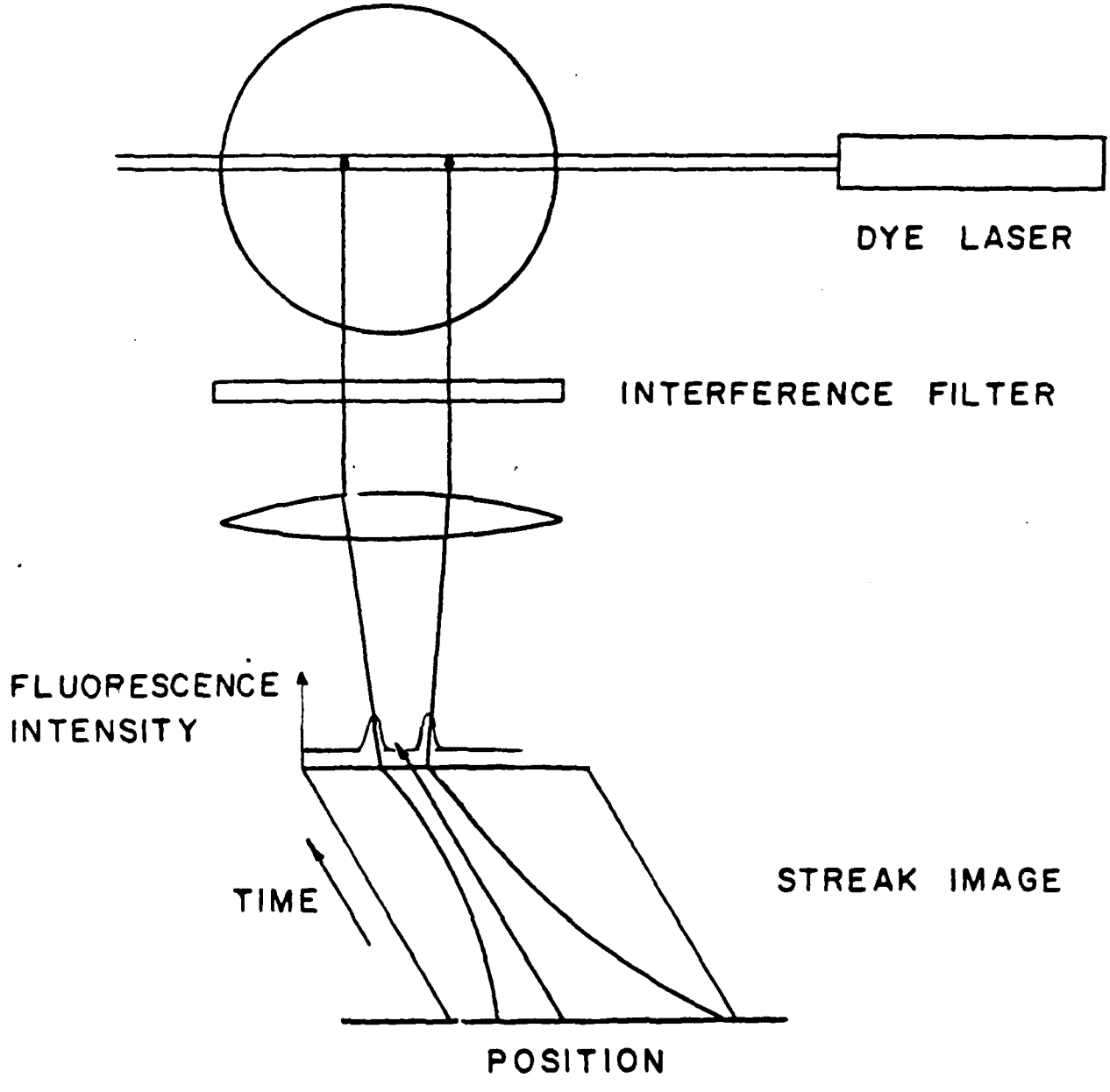

Figure 4. Spatially and temporally resolved $H = H_1$ contour using streak camera to record spatially resolved LIF intensity pattern.

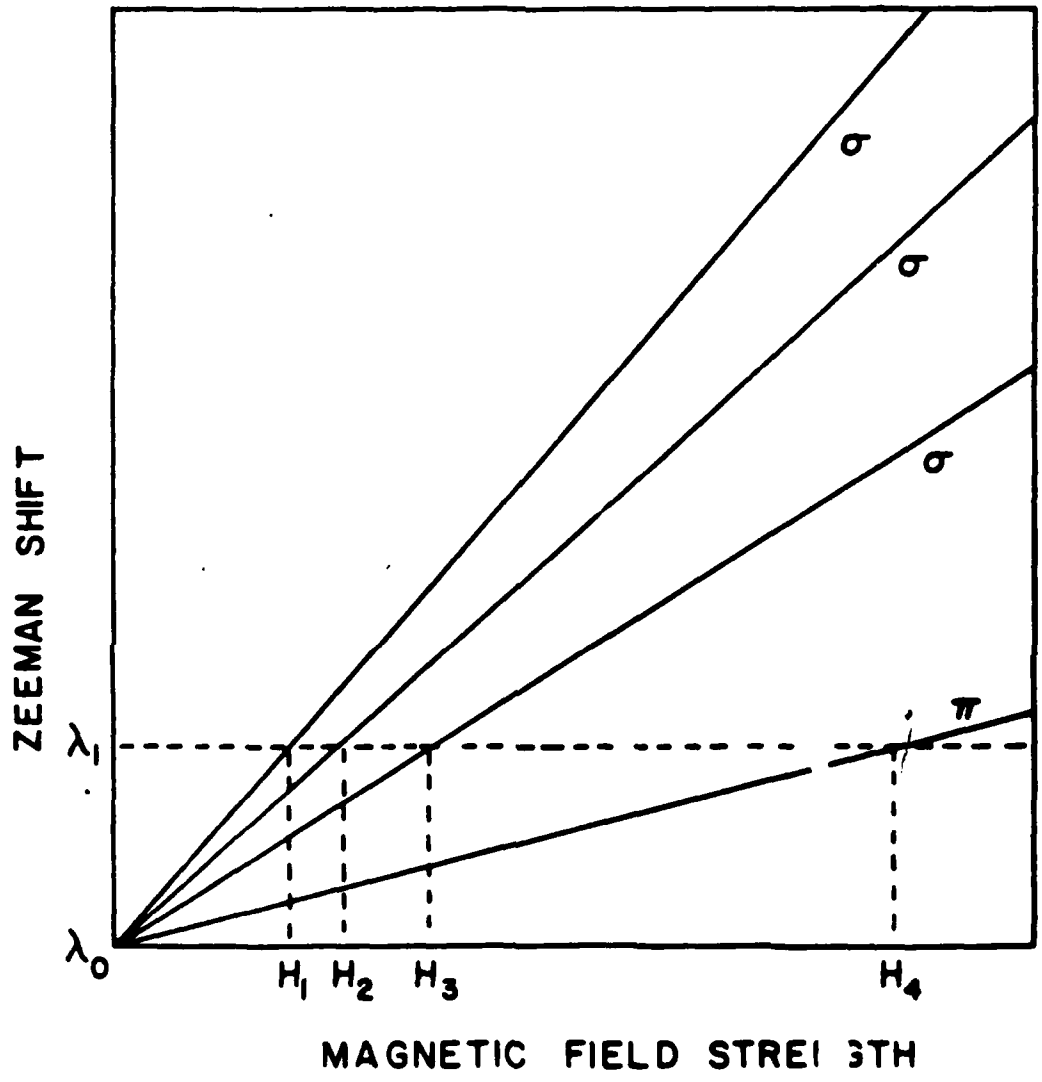

Figure 5. Magnetic fields probed by a single laser wavelength exciting the Zeeman split multiplet spectrum of the 566.66-nm transition in N II.

ACCESSIBILITY OF BEAM PLASMA CHANNEL TO LIF MEASUREMENT OF MAGNETIC FIELDS

The LIF technique pursued here for recording magnetic field contours requires the half width of the absorption line probed to be less than the Zeeman shift.

The dominant line broadening processes that must be considered are Stark broadening by electrons and ions and Van der Waals broadening by collisions with neutrals. The Stark broadening has been calculated by Griem (Refs. 6,7) and measured by others (Ref. 9). The full widths of the candidate lines at half intensity can be calculated using Griem's expression

$$\Delta\lambda_S = 2\left[1 + 1.75 \times 10^{-4}\, Ne^{1/4}\right] A \left[1 - 6.3 \times 10^{-4}\, \frac{N_e^{1/6}}{T_e^{1/2}}\right] 10^{-16}\, W\, N_e \qquad (4)$$

where T_e and N_e are the electron temperature (K) and electron number density (cm^{-3}) and the width W and parameters A are taken from the table in Ref. 7. The resulting values for Stark widths are presented in Table 1.

The Van der Waals broadening is more difficult to estimate because theoretical expressions for the broadening by different gases are not well developed and measurements are not available for the particular transition of interest (Refs. 10,11). Some estimates of the upper limit on the broadening of the 585.25-nm line of Ne by nitrogen can be made using the results of Kaliteevskii, et al (Ref. 12). They have used the Hanle effect to measure the frequency of depolarizing collisions for excited neon states by collisions with neon and helium atoms. These results are presented in Table 2 along with the results of Gubin, et al, who inferred the width of a transition in a HeNe laser by measuring the lasing threshold for a range of helium pressures and attenuators inserted into the lasing cavity (Ref. 13). Kielkopf indicated that depolarizing collisions are not necessarily effective line broadening processes and the above values would probably be upper limits (Ref. 8). Note that the higher lying levels (4P' and 5S') are broadening more than the lower lying levels, consistent with the observations on alkali metal atoms and the fact that helium is a more effective broadening agent than nitrogen or neon (except for $3S'[1/2]_1$ level) (Ref. 10). Also note that the two 3P' levels are broadened approximately the

same. Using these trends as a guide, the broadening of the 585.2-nm line by nitrogen will be less than the 38 kHz/Pa value observed for He, which translates into a line width $\Delta\lambda_p \simeq 4.365 \times 10^{-8}$ nm/Pa.

TABLE 2. WIDTH OF LOW LYING NEON ENERGY LEVELS DUE TO COLLISIONS WITH NEUTRAL PERTURBERS

LEVEL	PERTURBER	$\gamma \left[\frac{kHz}{Pa}\right]$	REF
$4p'[3/2]_2$	Ne	90 ± 15	5
	He	165 ± 15	5
$3P'[3/2]_2$	Ne	26 ± 3.7	5
	He	29 ± 4.5	5
$3P'[3/2]_1$	Ne	15.7 ± 5.3	5
	He	38 ± 7.5	5
$2S'[1/2]_1$	Ne	22 ± 3.7	5
	He	5.3 ± 1.5	5
$5S'[1/2]_1$	He	300	6

Information about the Van der Waals broadening of ion lines is limited. However, note that the Stark broadening of ion lines is generally less than the broadening of neutral lines (in some cases an order of magnitude less), and that the broadening of neutral lines by collisions with neutrals is smaller for the low-lying energy levels than for the higher levels. This is physically reasonable since an electron further from the core is more easily perturbed than a low-lying electron. This trend indicates that perturbation of ion lines by collisions with neutrals is expected to be less than in the case of neutral emitters (Ref. 8). If the Van der Waals broadening of the nitrogen ion line is taken to be an order of magnitude less than broadening of the neutral NeI 585.25-nm line, it can be ignored in the subsequent analysis.

The LIF contour technique requires the line width to be less than Zeeman shift, with the minimum resolvable field corresponding to equality between these two quantities. The region of accessability of the LIF technique on a beam-plasma system has been estimated by determining at what positions the Zeeman shift is equal to the line broadening. For these calculations the electron densities and magnetic field profiles calculated by R. Lemke (Ref. 14) were used. For a range of radial positions, the Stark broadening, Zeeman shift (0.00165-nm/kg) and neutral broadening were calculated. At 84 kPa, Stark broadening exceeds Zeeman shift for $r \leq 1.2$ cm, and neutral broadening exceeds Zeeman shift for $r \geq 1.7$ cm. The accessible region is shown striped in Fig. 6. At 8.4 kPa only the interior ($r \leq 0.75$ cm) is unaccessible due to Stark broadening, with neutral broadening negligible to r = 5 cm (Fig. 7).

These calculations indicate that at low pressure most of the current plasma channel can be diagnosed using the LIF technique to fluoresce the 585.25-nm line of NeI. However, at atmospheric pressure, Stark and neutral broadening limits the accessible region to a small fraction of the plasma volume.

For the candidate ion lines, only the inner $r \leq 0.25$-cm region of the plasma column is inaccessible to probing. The region to the right of the solid line in Figs. 6 and 7 can be probed until the magnetic field decreases to the value where Van der Waals broadening (not considered in this case) limits the resolution at large values of r.

DETECTABILITY OF LIF SIGNALS

LIF signal amplitude--To determine what fraction f of the gas must be neon to produce a detectable signal, the magnitude of the LIF signal must be calculated and compared with the beam induced background radiation intensity within the pass band of the interference filter. The relationship of the fluorescent intensity to the number density $N(i)_o$ of atoms in the lower state of the transition is presented next.

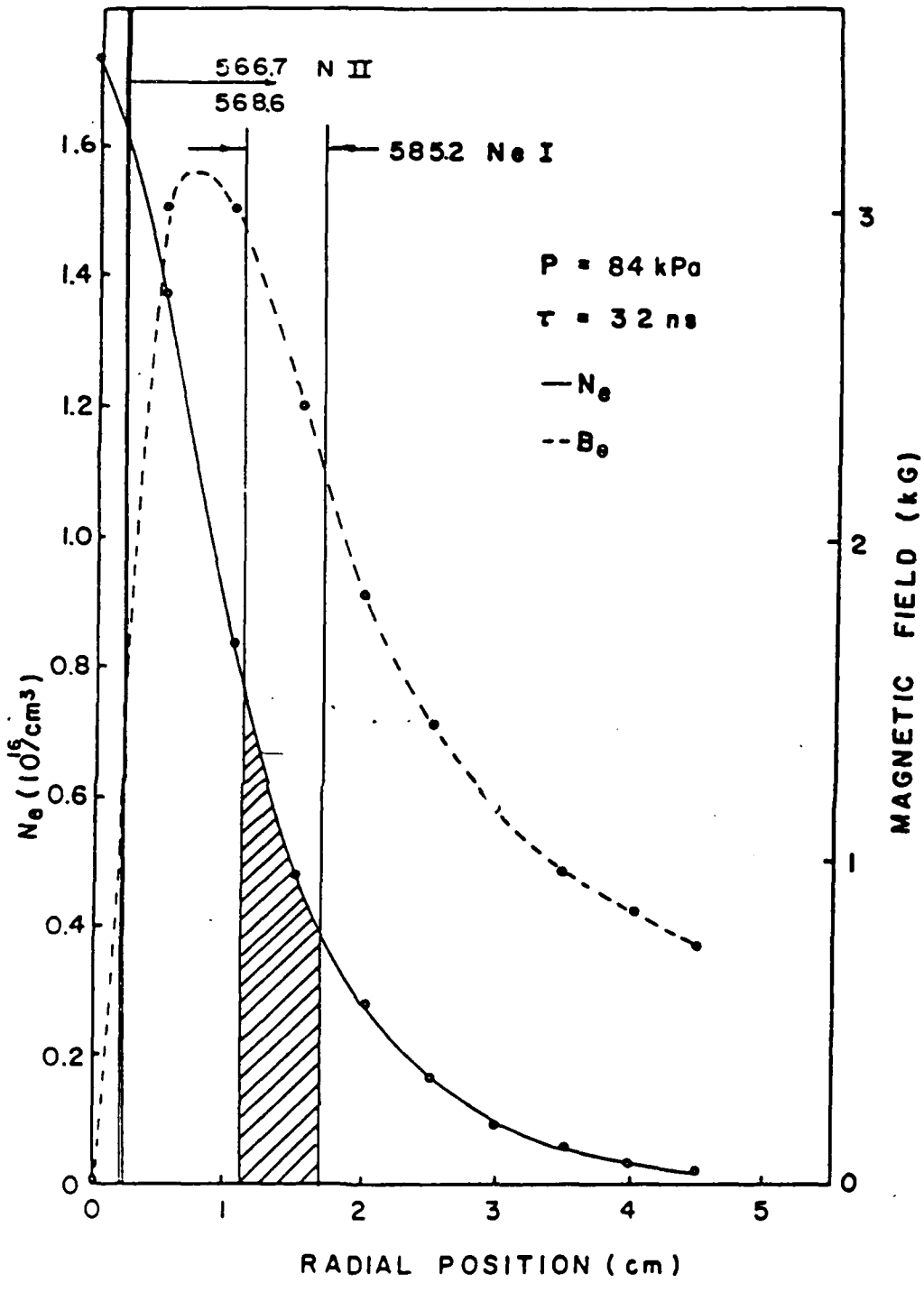

Figure 6. Regions of accessibility to magnetic field measurements on a 20-kA REB using LIF for the 585.2 line of neutral neon (shaded area) and the 566.7 and 568.6-nm lines of ionized atomic nitrogen (to the right of the double verticle lines).

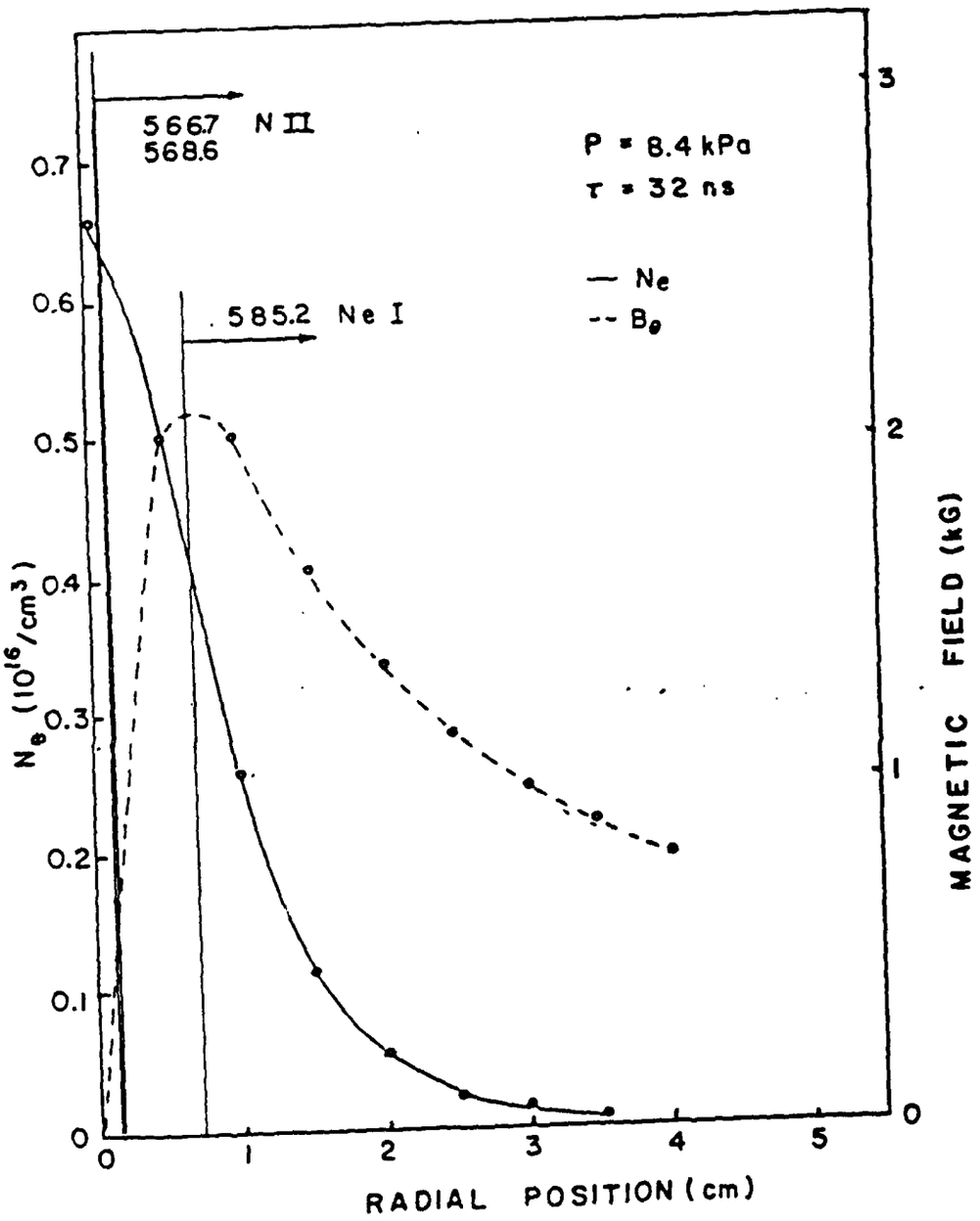

Figure 7. Regions of accessibility to magnetic field measurements on a 20 kA REB using LIF. (Radial positions to the right of the vertical lines can be probed using the atomic transitions designated.)

The derivation draws on the work of Razdobarin et al (Ref. 1) and Daily (Ref. 16). The number density of atoms in the upper state is determined by the rate equation

$$\frac{dN(j)}{dt} = N(i)B_{ij}U_o - (Q_j + A_j + B_{ji}U_o)\ N(j) \tag{5}$$

where the first term represents upward transitions induced by the pumping dye laser and the second term the total depopulation rate. Here B_{ij} and B_{ji} are the Einstein coefficients for absorption and stimulated emission, A_j is the total Einstein coefficient for spontaneous emission summed over all transitions, Q_j is the total collisional deexcitation rate and U_o is the laser energy density/unit frequency interval. The steady-state population density of the upper state is given by the expression

$$N(j) = \frac{B_{ij}U}{Q_j + A_j + B_{ji}U_o}\ N(i) \tag{6}$$

If the pumping laser is sufficiently intense for stimulated emission to overcome collisional depopulation processes, i.e.,

$$B_{ji}\ U_o \gg Q_j + A_j \tag{7}$$

then two important features of the laser induced fluorescence technique emerge. First of all, Eq. 6 simplifies to

$$N(j) = \frac{B_{ij}}{B_{ji}}\ N(i) \tag{8}$$

which is known as the saturated condition. This results in a very simple relationship between the fluorescence intensity and the number density of atoms in the state N(i) as follows. The principle of detailed balance ($g_iB_{ji} = g_iB_{ij}$) can be used to simplify Eq. 8 to

$$N(j) = \frac{g_j}{g_i} \quad N(i) \tag{9}$$

where g_i, g_j are the degeneracies of these two levels. The intensity of the fluorescence radiation is given by the relation

$$U_{LIF} = \frac{h\nu A_{ji}}{4\pi} \frac{g_j}{g_i} \quad V_{LIF} \quad N(j)\Omega \tag{10}$$

where Ω is the solid angle subtended by the collection optics and V_{LIF} is the volume of the region excited by the laser viewed by the collection optics. The intensity of the fluorescence radiation can be related to the undisturbed number density, $N(i)_o$, under the simplifying assumption that the total population of the two states is not altered

$$N(i)_o + N(j)_o = N(i) + N(j) \tag{11}$$

This reduces to the condition $N(i)_o \cong N(i) + N(j)$ if the upper state is not heavily populated $[N(i)_o >> N(j)_o]$. In this case the fluorescence radiation intensity is given by

$$U_{LIF} = h\nu \frac{A_{ji}}{4\pi} \quad V_{LIF} \left[1 + \frac{g_i}{g_j} \right]^{-1} \Omega \quad N(i)_o \tag{12}$$

which is independent of the collisional deexcitation rate or the intensity of the excitation laser.

The condition represented by Eq. 7 alters the response of the LIF technique relative to the frequency response of emission spectroscopy that is very important to pulsed applications. This can best be seen by comparing the time constants for light emission observed in these two applications. Equation 5 without the absorption and stimulated emission terms reduces to the expression

$$\frac{dN(j)}{dt} = -(Q_j + A_j)\ N(j) \tag{13}$$

which is a homogeneous differential equation with the solution

$$N(j) = N_o(j)e^{-t/\tau} \tag{14}$$

$$\text{where} \quad \tau = \frac{1}{Q_j + A_j} \tag{15}$$

This limit of Eq. 5 describes the temporal response of the radiation observed in emission spectroscopy having a minimum temporal resolution given by Eq. 15. The temporal response of the LIF technique in the saturation limit (Eq. 7) is given by the expression

$$\frac{dN(j)}{dt} + B_{ji}U_oN(j) = B_{ij}U_oN(i) \tag{16}$$

which has a characteristic time constant given by

$$\tau = \frac{1}{B_{ji}U_o} \tag{17}$$

that can be made arbitrarily small. Equation 17 points out one of the important advantages of the LIF technique over emission spectroscopy. In emission spectroscopy, the temporal response is determined by the lifetime of the upper state, which is determined by the radiative lifetime or collisional quenching rate. With LIF, the lifetime of the upper state can now be controlled by the stimulated emission which has a time constant (Eq. 17) at the disposal of the investigator. The temporal advantage of the LIF technique is not without its drawbacks. The saturation condition given by Eq. 7 requires high laser powers, which in turn can perturb the plasma.

BACKGROUND INTENSITY

The background emission comes from two sources, 585.2-nm emission due to beam excitation of the upper level of the transition and the beam-excited fluorescence of other emission in the pass band of the detector. The beam-excited 585.2-nm intensity is given by the expression

$$U_P = h\nu \frac{A_{ji}}{4\pi} \Omega V_P N(j)_o \tag{18}$$

where V_P is the plasma volume seen by the collection optics. A nonequilibrium analysis of the air chemistry is required to determine the population levels $N(i)_o$ and $N(j)_o$ that contribute to the radiation of interest. Although this is out of the scope of the present study, an estimate of the relative magnitude of the population levels in the $1s_2$ and $2p_1$ states of neon can be determined by considering only direct beam excitation processes and ignoring secondary electron excitation and cascade processes. In this approximation the population of the $1s_2$ level of neon is obtained by equating the beam excitation rate to the collisional quenching rate, i.e.,

$$\sigma \frac{J}{e} N(o)_n = K N(i)_o N_A \tag{19}$$

Here $N(o)_n$ is the density of ground state neon atoms and N_A is the background air density. The two-body transfer to nitrogen is taken to be the dominant deexcitation process, with the rate constant for depopulating the $1s_2$ resonance state taken to be the same as the value 8.1×10^{11} cm^3/s obtained by Yokoyama, et al, for depopulating the $1s_4$ resonance state (Ref. 16). The deexcitation rate by oxygen is taken to be two-thirds of the nitrogen value (Ref. 17). The cross section for exciting the $1s_2$ level has been estimated by extrapolating the value observed by Miers, et al (Ref. 18), at 100 eV using the energy dependence for σ obtained by Peterson and Allen (Ref. 19).

$$\sigma(E) = C [1 - W_j/E]^2 E^{-0.75} \tag{20}$$

Here W_j is the energy required to excite the j^{th} state, E is the electron energy, and C is a constant. The value of σ obtained with this extrapolation procedure is 3.1×10^{-21} cm^2 for 10 MeV electrons. The density of $1s_2$ state is estimated to be $1.84 \times 10^{11}/cm^3$ for a 1-cm radius, 20-kA beam propagating in an air-neon mixture at 84 kPa containing 10 percent neon. The LIF intensity is readily calculated using Eq. 12 and the results are presented in Table 3. The beam induced 585.2-nm fluorescence intensity is estimated using Eq. 18 and the Boltzmann expression

$$\frac{N(j)_o}{N(i)_o} = \frac{g_j}{g_i} \exp -\Delta E/KT_{ex} \tag{21}$$

relating the $1s_2$ and $2p_1$ states separated by $\Delta E = 2.118$ eV. Numerical studies of the beam-air chemistry have indicated that the gas atoms have an excitation temperature, T_{ex}, whose value is approximately 0.8 of the electron temperature (Ref. 20). These studies estimate the electron temperature to be 0.6 – 0.7 eV for a 1 to 2-cm-diam beam. The value of the background beam-induced 585.2-nm fluorescence obtained with Eqs. 18 and 21 is presented in Table 3.

TABLE 3. LASER-INDUCED AND BACKGROUND FLUORESCENCE FOR A 10-MeV, 20-kA BEAM PROPAGATING IN 84 kPa AIR WITH 10 PERCENT NEON

LIF	Beam Induced		EN
	Neon	Air	
U_{LIF}	U_p	U_b	
$0.089\ V_{LIF}\ \Omega$	$0.0014\ V_p\ \Omega$	$0.0092\ V_p\ \Omega$	2.65

The magnitude of the 585.2-nm background intensity must be added to the beam excited fluorescence emitted by the air component of the gas. This latter quantity can be estimated using the measurements of Davidson and O'Neil for the efficiency of an electron beam in generating fluorescence in air (Ref.

21). They found that the power radiated per unit frequency interval can be related to dE/dX, the power deposited per unit volume by the beam in the gas, by the expression

$$U_b = \eta \frac{dE}{dX} \frac{J_b}{e} \frac{V_P}{4\pi} \Omega \tag{22}$$

Here dE/dX is given by the Bethe expression

$$\frac{-dE}{dx} = \frac{2 N_A Z \pi e^4}{mv^2} \ln \left[\frac{\frac{mv^2}{2} E}{(1 - \beta^2) W} \right] \tag{23}$$

where Z is the number of electrons/atom, W is the excitation energy, E the beam energy, N_A the background gas density, and $\beta = v/c$. Davidson and O'Neil found that most of the radiation is emitted in the blue-violet range (Fig. 8), with a flat spectrum in the vicinity of the 585.2-nm line. They quote an efficiency of $\eta \simeq 0.12 \times 10^{-7}$ for the 585.4-nm line which can be used for the wavelength range of interest. The values of U_b calculated in this fashion appear in Table 3.

The bremsstrahlung emission by the plasma electrons has been estimated using the relationship given by Sheffield (Ref. 22).

$$P d\Omega \, d\lambda = 2.1 \times 10^{-36} \, g \, Z^2 \left[\frac{N_e N_i}{\lambda^2 Te^{1/2}} \right] \exp \left[\frac{-(1.2 \times 10^{-4})}{\lambda T_e} \right] V \frac{d\Omega}{4\pi} d\lambda \tag{24}$$

where V is again the volume viewed by the detector optics and g the gaunt factor. The power radiated per unit volume is 1.7×10^{-6} to 1.7×10^{-2} W for N_e in the range of 10^{14} to 10^{16}. These values are much less than the fluorescent values and can be ignored.

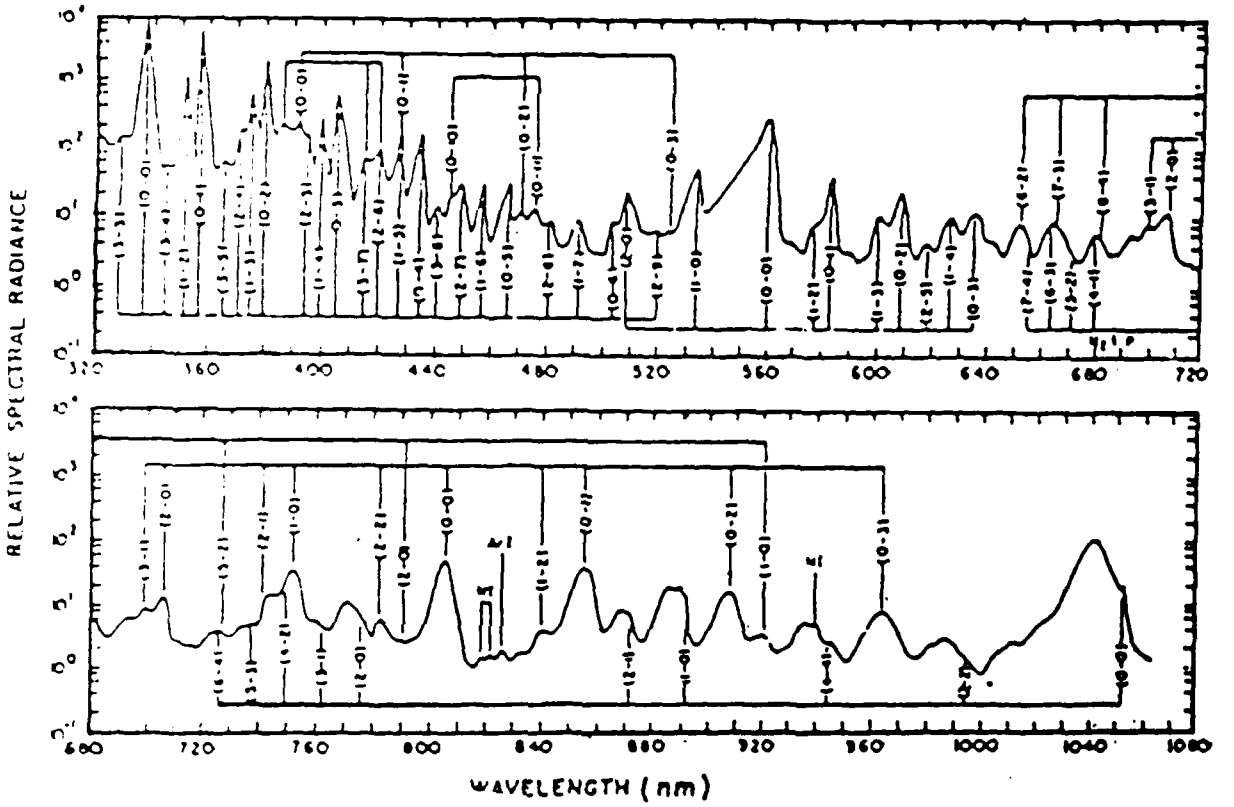

Figure 8. Relative spectral radiance of nitrogen at 80 kPa excited by 50-keV electrons (Ref. 22).

The ability to discern the image of the contour relative to the plasma emission depends on the relative intensity on and off the contour. This can be expressed as an enhancement factor

$$EN = \frac{U_{LIF} + U_p + U_b}{(U_p + U_b)} \tag{25}$$

where the relative magnitude of V_p and V_{LIF} can be estimated from Fig. 9. The plasma emission from the entire plasma cord intercepted by the collection optics contributes to V_p, whereas the LIF radiation is collected only from the intersection of the laser beam and the collection optics (shown striped). The enhancement has been estimated for a laser beam diameter of 0.4 cm and a plasma diameter of 2 cm and the results are presented in Table 3. The intensity of the contour stripe will be 2.65 times the intensity of the background light level. Only the spatial extent of the enhanced region is of interest in these studies because the magnitude of the field is determined by the dye laser frequency. A microdensitometer can resolve a 10 percent change in optical density on the film, which is more than an order of magnitude less than the anticipated enhancement. These contours should be readily discernible in a beam propagation experiment with a modest 10 percent addition of neon. An enhancement factor of 15 is anticipated in a pure neon propagation experiment.

EXCITATION TEMPERATURE MEASUREMENTS USING LIF

If the beam-generated fluorescence of the nitrogen and oxygen components of the mixture is small compared to the neon components and can be neglected in Eq. 25, then the excitation temperature can be estimated from the relative enhancement of the LIF signal. Substituting Eq. 12 for U_{LIF} and Eq. 18 for U_p in Eq. 25 and rearranging, the following expression for the excitation temperature is obtained

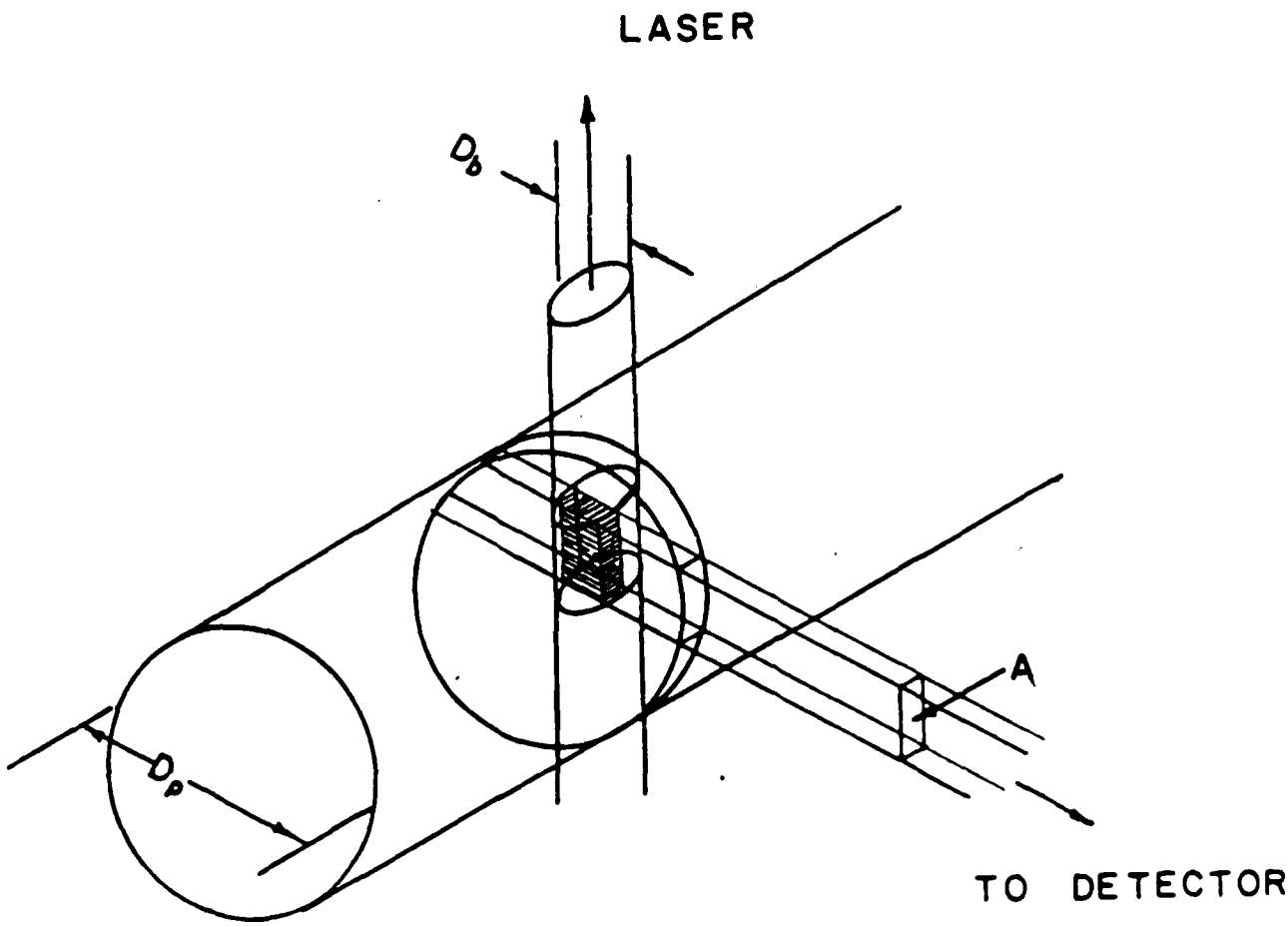

$$V_p = D_p A \qquad V_{LIF} = D_b A$$

Figure 9. Relationship of fluorescence volume, V_{LIF}, subtended by detector optics to plasma radiating volume, V_p, contributing to background intensity.

$$T = \frac{\Delta E}{\ln\left[\frac{g_i + g_j}{g_i}\left[\frac{(EN - 1)\, V_p + V_{LIF}}{V_{LIF}}\right]\right]} \qquad (26)$$

where EN is the ratio of the emitted radiation with laser present to the background level. This expression can be used to infer the electron temperature from relative intensity measurements if the transition is saturated (Eq. 7).

III. HIGH CURRENT DISCHARGE SYSTEM

The proof-of-principle experiments were carried out on the discharge system shown schematically in Fig. 10. The positively charged capacitor was connected to the high voltage electrode via a spark gap switch and the return current flowed in a 6.5-cm-diam copper tube surrounding the 4.4-cm-diam discharge tube. Studies were carried out using 4.4-cm-diam disc electrodes and 1.27-cm-diam pointed rod electrodes. The electrode separation was varied from 5 to 28 cm. The current was monitored using a T & M model CT-6.5 current probe and the voltage at the high voltage electrode was measured with the 10^4 to 1 divider, shown in Fig. 10. A cylindrical Langmuir probe was inserted axially through the center of the low voltage electrode to measure the plasma properties.

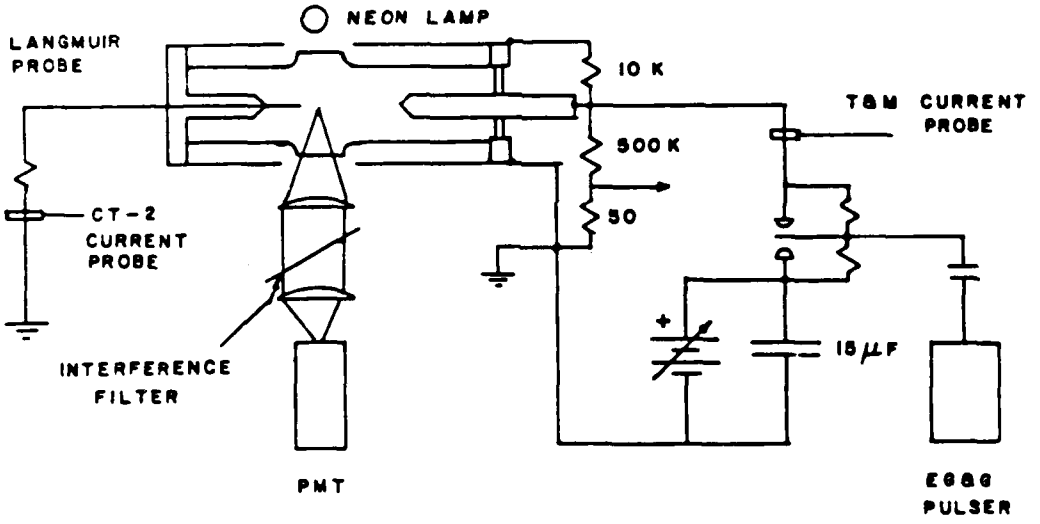

Figure 10. Schematic of discharge tube and related circuitry.

The current waveform was measured for a range of capacitor voltages and backfill pressures and compositions. The inductance and resistance was inferred from the oscillation period (18.5×10^{-6} s) and current decay rate to be 0.577×10^{-6} H and 0.025 Ω, respectively. Since the estimated inductance of the plasma is small and the circuit is underdamped, the oscillation period is relatively independent of electrode configuration or discharge condition.

The value of the current at the first peak (1/4 period) in neon and in nitrogen is presented as a function of the initial voltage on the capacitor in Fig. 11. The neon results are a composite for different backfill pressures. The slope of the strainght line extrapolated to zero time for the measurements (I/V = 4.71) agrees well with value predicted for I/V (5.10) based on the equivalent LRC circuit and the value of L deduced from the period of oscillation. These results indicate that the current probe is calibrated to within 8 percent.

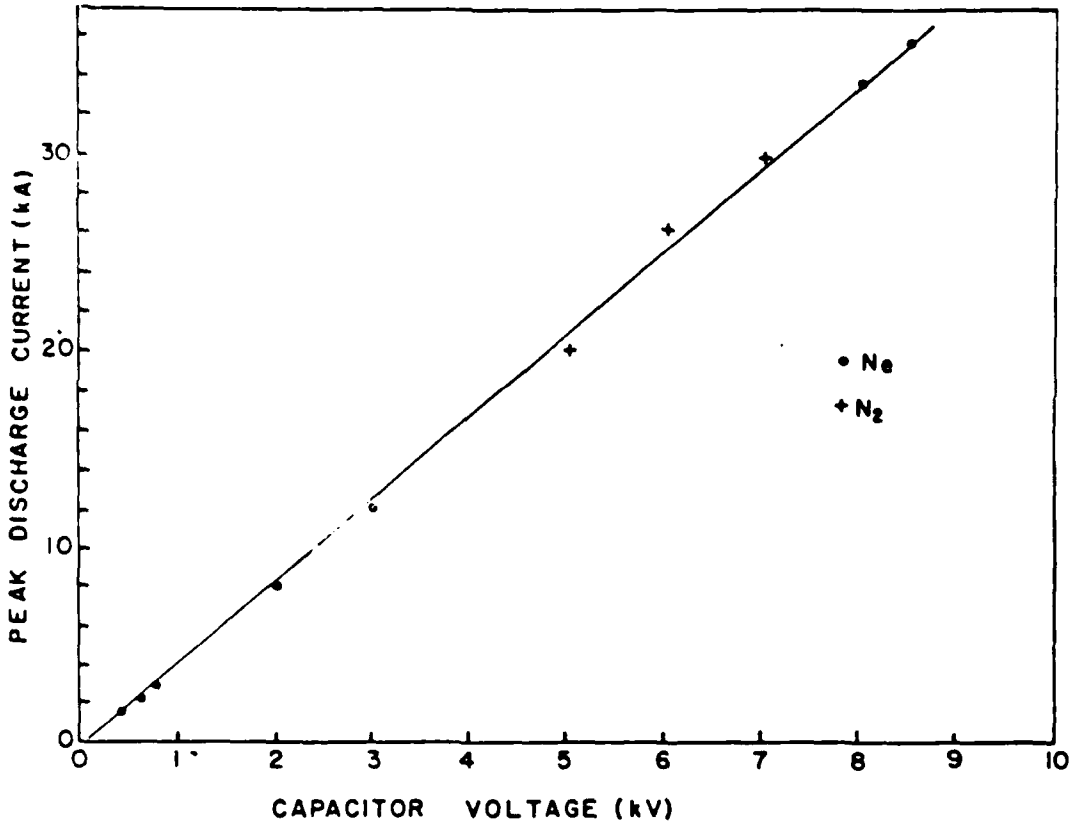

Figure 11. Dependence of peak discharge current on capacitor voltage for neon pressures from 130 to 660 Pa and in 130 Pa of nitrogen.

Langmuir probe measurements of the plasma characteristics were made using self biased and externally biased configurations. In the self biased mode, a Tektronix CT-2 probe measures the current flowing in a resistor connecting the probe to ground. Measurements are made for a range of resis-

tor values, and the data is analyzed by measuring the current flowing at a particular time in the discharge. The probe bias is taken to be the product of the probe current and resistor value. No probe currents were observed during the first, third, etc., half cycle of the current oscillation when the high voltage electrode was positive relative to the low voltage electrode. Measurements obtained during the second half cycle when the low voltage electrode was positive are shown in Fig. 12. Externally biased probe measurements were made using a d.c. power supply shunted by a 1-μF capacitor and the CT-2 current probe. Measurements made on the second half cycle yielded results similar to those in Fig. 12. Measurements on the fourth half cycle are presented in Fig. 13. The results indicated that space potential is approximately 90 V negative with respect to ground during the second half cycle, and approximately 4 V negative during the fourth half cycle when these measurements were made. During the even half cycles, the low voltage electrode is the anode, and space potential in the positive column is expected to be close to the voltage of this electrode. The differences observed during the second and fourth half cycles can be attributed to inductive effects, since the low voltage electrode is connected to ground through the plasma inductance, but quantitative correlations have not been made. The results indicate that the electron temperature is small (few tenths of an eV) and that the product of electron density and the square root of electron temperature (eV) is approximately 1 to 3 x 10^{13}. Measurements at 3 kV on a 533-Pa neon discharge gave saturation currents and hence electron densities an order of magnitude larger than this. The analysis did not include any magnetic field effects since field strength information is not available and the on-axis field is expected to be small.

The emission profile was measured by scanning a pinhole perpendicular to the discharge axis and Abel inverting the recorded intensity distribution. Figure 14 presents the radial intensity distribution in a 2-kV discharge 2 μs into the pulse. The results indicate that the radial emission profile is an annular ring 2.2-cm outer diameter. Since the radiation is primarily from the neutrals (ion lines could not be measured at this current), it is not clear if the current density profile is proportional to the emission profile. The current could be flowing in a 0.4- to 0.5-cm-radius channel within the annulus where the ionization of the background gas has

reduced the neutral emission intensity. Measurements at higher currents and voltages (36 kA, 10 kV in 40 Pa N_2) reveal a very bright arc 0.7 cm in diameter. The emission intensity of the 585.25-nm NeI line measured at different radial positions reaches a peak value at progressively later times as the distance from the center increased. These results indicated that a 36-kA discharge in neon, at a pressure of 13 Pa, produces a pinched column that then expands with a velocity of approximately 2×10^6 cm/s. The emission in this case is primarily ionic and a number of N II lines have been measured. These are described below.

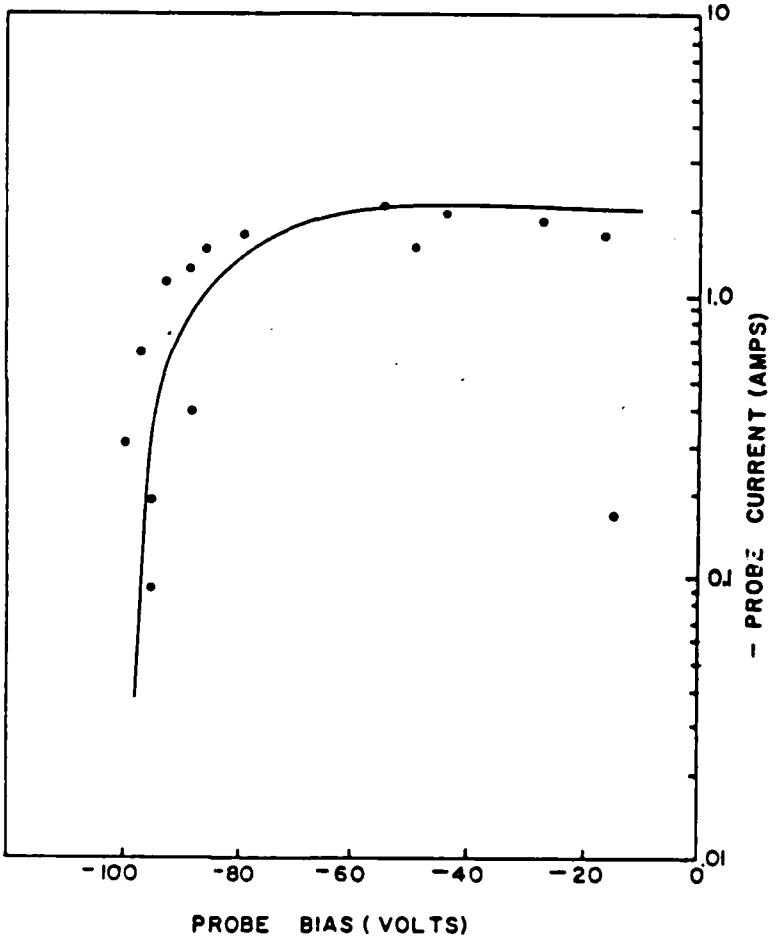

Figure 12. Current-voltage characteristics of a self-biased Langmuir probe. (Probe voltage is product of probe current and resistance connecting probe to ground. Measurements in second half current cycle of 2-kV discharge in 530 Pa of neon.)

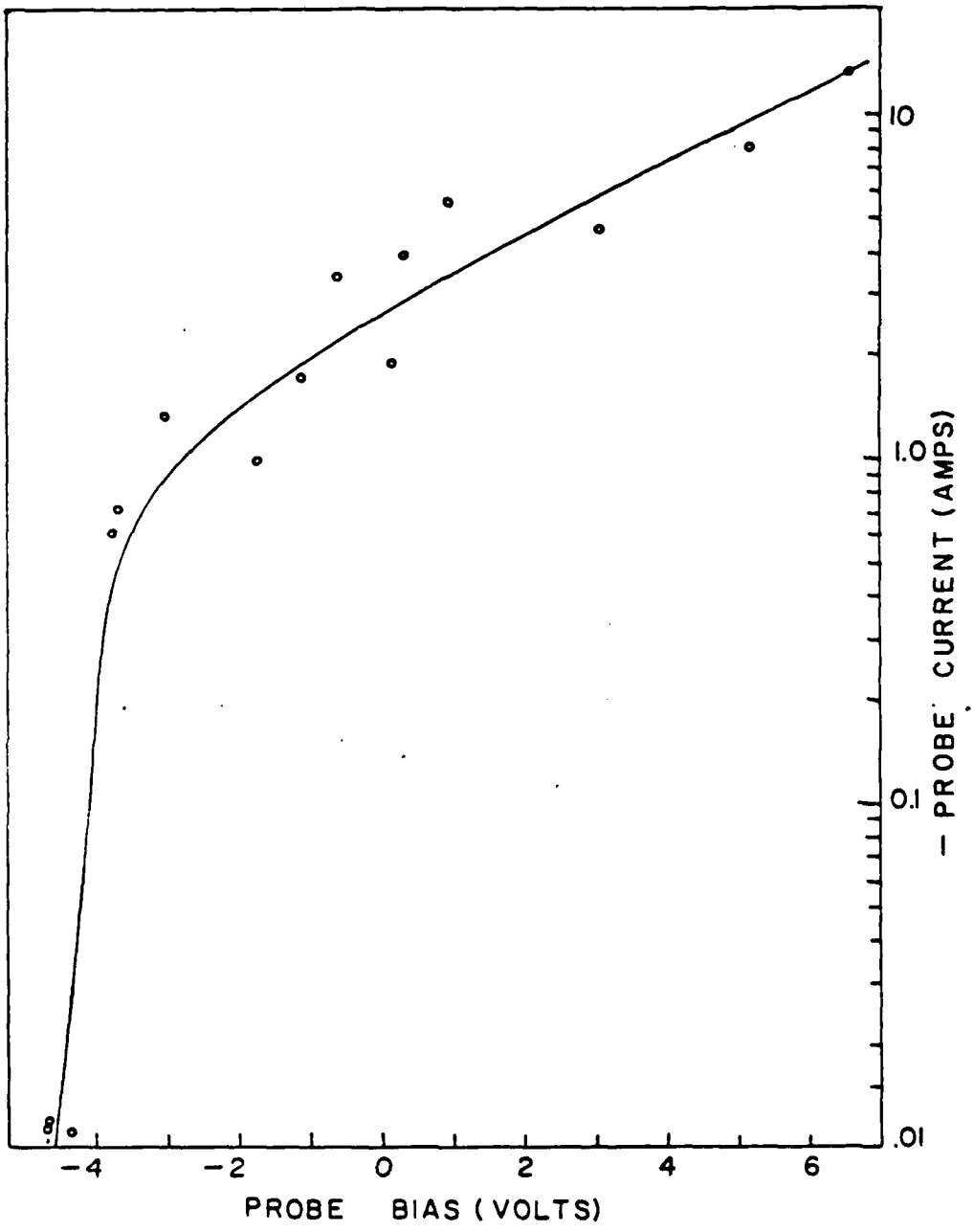

Figure 13. Current voltage characteristics of biased probe in fourth half-current cycle of 2-kV discharge in 530 Pa of neon.

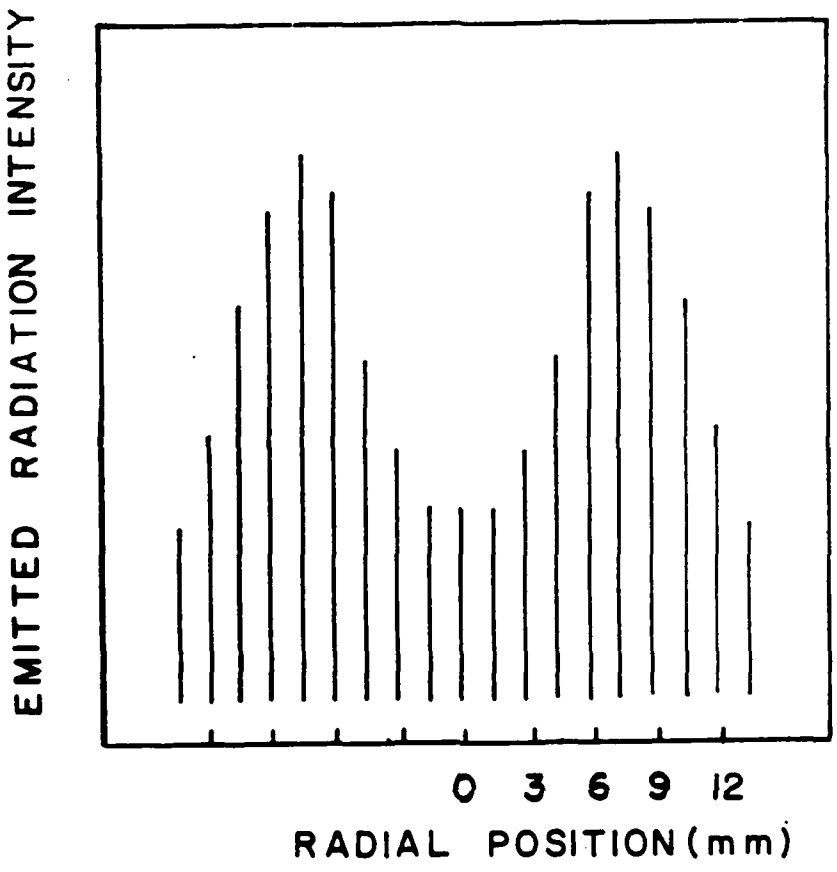

Figure 14. Radial distribution of unfiltered emission from a 2 kV discharge in 530 Pa of necn.

Emission line profiles were measured using an optical fiber to couple the collection optics to a monochrometer. The line profile was recorded by measuring the emission intensity for a number of wavelength settings of the monochrometer. The measurement at each setting was normalized for shot-to-shot variation using the signal from a PIN diode monitoring the overall emission intensity. The line profiles for the 566.66, 517.95, and 444.7 nm lines of atomic nitrogen are shown in Fig. 15. The intensity of a given line depends on the population of the upper state (2) of the transition according to the relationship

$$I_{21} = \text{constant} \frac{1}{U(T)} \frac{g_2 A_{21}}{\lambda_{21}} e^{-E_2/KT} \quad (27)$$

where U(T) is the total partition function at temperature T. This can be rewritten as

$$\ln \left[\frac{I_{21} \lambda_{21}}{g_2 A_{21}} \right] = \text{const} - E_2/KT \quad (28)$$

from which the excitation temperature T can be inferred. The line emission data, corrected for the response of the photomultiplier and the linear regression fit of the data to Eq. 28, yield a value of 3.5 eV for T. The plasma density inferred from the Stark broadening of the 566.66-nm line is $3.7 \times 10^{17}/cm^3$.

The dependence of the excitation temperature on the backfill pressure of nitrogen was studied by measuring the relative intensity of two transition multiplets. These are the lines from 517.15 nm to 518.03 nm corresponding to the $^5P^o - {}^5D$ and $^5D^o - {}^5F$ transitions and the 566.66-nm transition. For these measurements, the slits on the monochrometer were opened wide enough to measure all of the lines in the multiplet but were narrow enough to exclude others. Measurements were of the on-line intensity and adjacent continuum intensity for each line at each pressure. The temperatures were deduced from the ratio of the intensities of these lines using Eq. 28. These lines were chosen because the intensity ratio is related to the energy level difference and this difference was the maximum that could be studied using the current detection system. Figure 16 presents the results for times corresponding to the peak currents in the first and second half cycle. The temperature appears to be slightly lower during the second half cycle, but there is no significant variation with pressure over the range studied.

Because of insufficient intensity, the emission line profiles could not be studied at lower capacitor voltages and arc currents where most of the LIF studies were conducted.

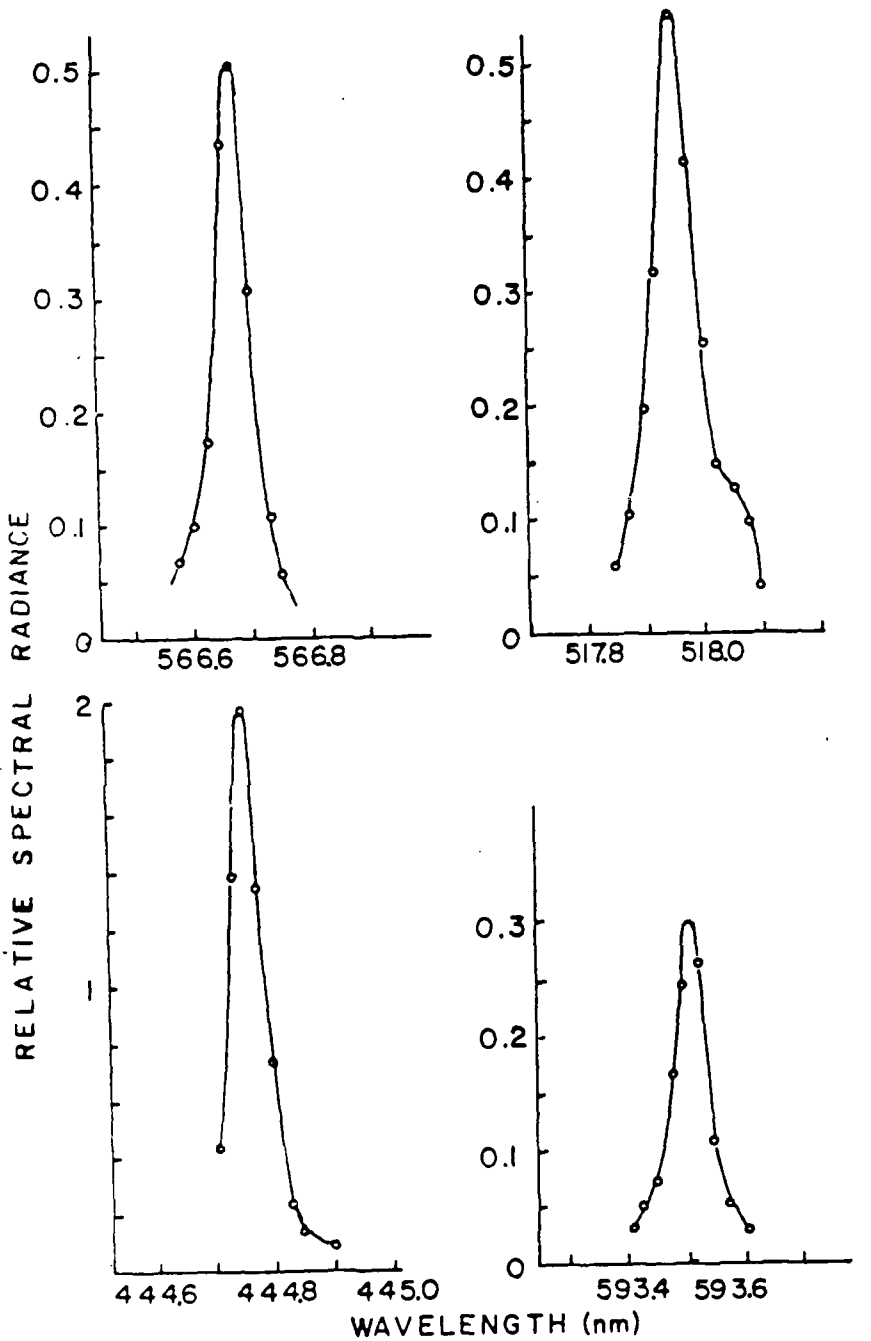

Figure 15. Emission spectra of four nitrogen ion lines obtained with a monochrometer having a resolution of 0.02-nm in a 8.5-kV discharge in nitrogen at 0.4 kPa.

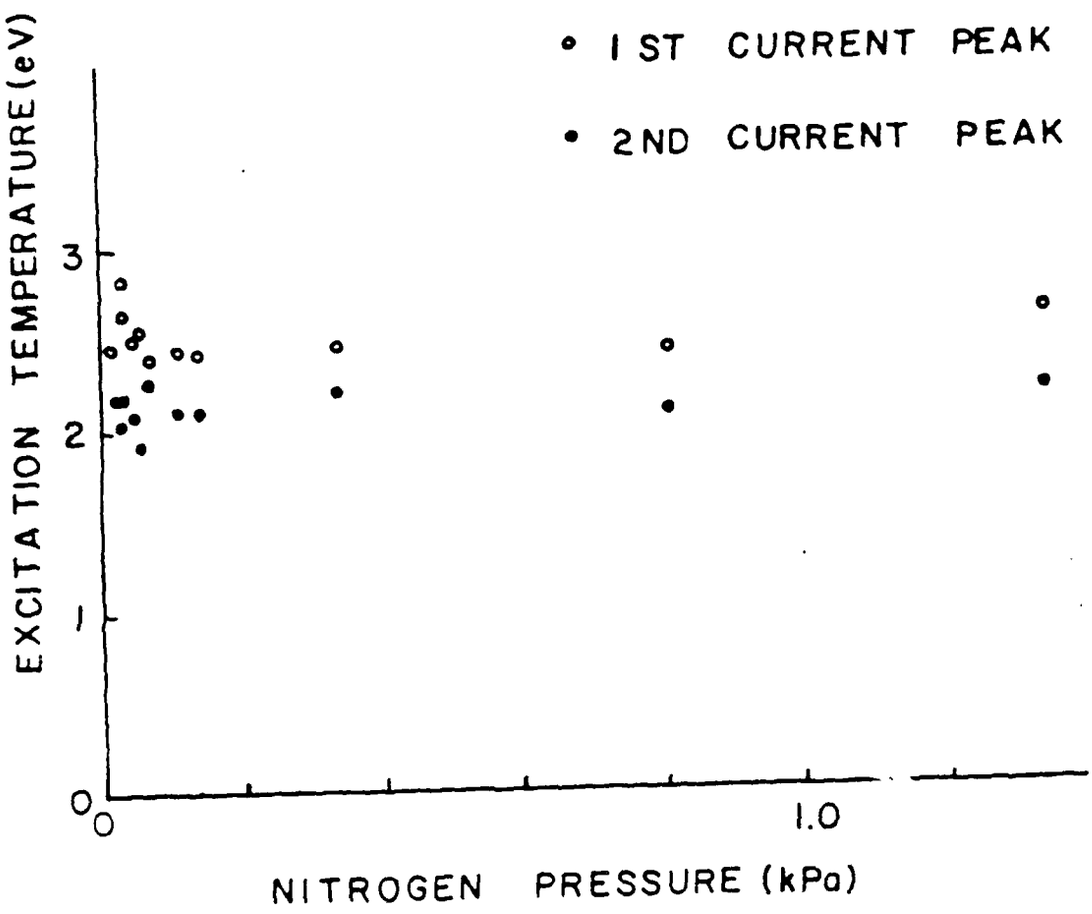

Figure 16. The excitation temperature inferred from the intensity ratio of singly ionized ionic lines in an 8.5-kV discharge.

IV. LASER-INDUCED FLUORESCENCE STUDIES ON THE 585.25-nm LINE IN NEON

EXPERIMENTAL SETUP

The experimental setup used for these studies is shown in Fig. 17. The 50/50 beam splitter directs half the laser output to a set of mirrors which pass the beam perpendicular to the plane of the paper through the discharge tube. The fluorescent radiation is viewed by two lenses which image the centerline of the discharge onto an aperture at the focal plane of the second lens. An interference filter with a bandwidth of 1.6 nm is located in the collimated beam between the two lenses, and the radiation is detected by a photomultiplier tube. The other half of the beam is monitored with PIN diodes, monochrometers, and a Fabry-Perot spectrometer to assess the laser output using a series of glass plates as beam splitters (approximately 5%). The PIN diode signal is a measure of the laser output power used to normalize the data to take into account variation in laser power level. The monochrometer, having a resolution of 0.02 nm, is used to roughly calibrate the laser tuner. This is done by first setting the monochrometer to the centerline frequency of the transition using a neon lamp. Next, the radiation amplitude passed by the monochrometer is measured, since the micrometer drive, which tilts the mirror on the grazing incidence tuner, is varied (see Fig. 17). Small changes in laser frequency and the line width of the laser output are measured using the Fabry-Perot spectrometer. A more detailed view of the discharge tube and collection optics is shown in Fig. 10. A movable aperture at the focal plane of the second lens is used to measure the spatial distribution of the LIF radiation. The narrow band interference filter is tilt-tuned to pass the 585.25-nm radiation using a neon lamp located at a chamber port on the opposite side of the discharge tube. The filter is rotated until a peak in the photomultiplier output is achieved. The linear response range of the photomultiplier was checked by measuring the amplitude of the detected signal as the discharge intensity was varied using neutral density filters. All fluorescence measurements were restricted to the linear regime.

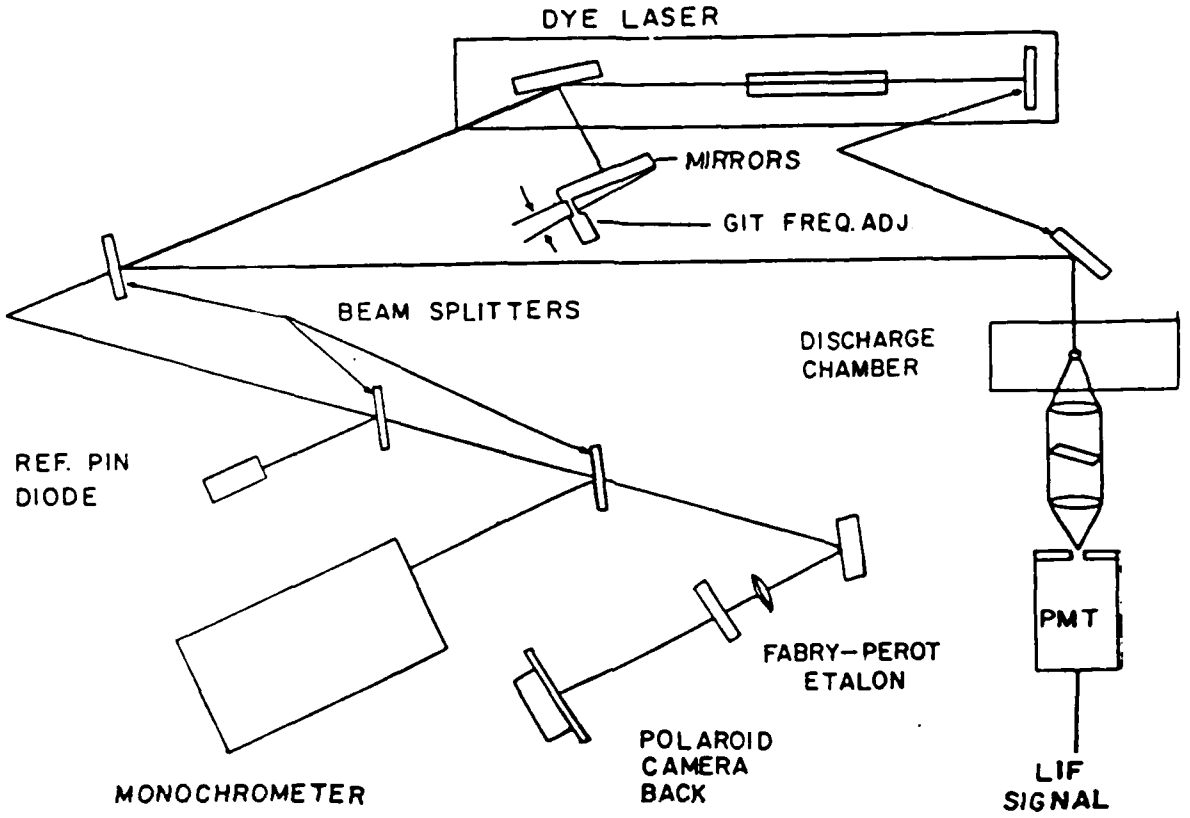

Figure 17. Schematic view of experimental set-up for measuring LIF on a pulsed discharge system.

LASER PERFORMANCE

The wavelength of the laser radiation has been measured with a monochrometer for a series of settings of the grazing incidence tuner (GIT) micrometer drive. The results shown in Fig. 18 indicate that the laser wavelength is proportional to the micrometer drive of the GIT with a slope of 9.11 $\pm$ 0.5 nm/mm. These monochrometer measurements are adequate for roughly tuning the laser, but the 0.02-nm resolution of the monochrometer limits its utility in measuring small wavelength changes or determining the laser line width. A Fabry-Perot interferometer has been used to complement the monochrometer measurements. The free spectral range of the Fabry-Perot (FP) etalon was calibrated by measuring the diameter of the FP ring pattern generated by a HeNe laser as the lens-to-film plane distance was varied. This is described below.

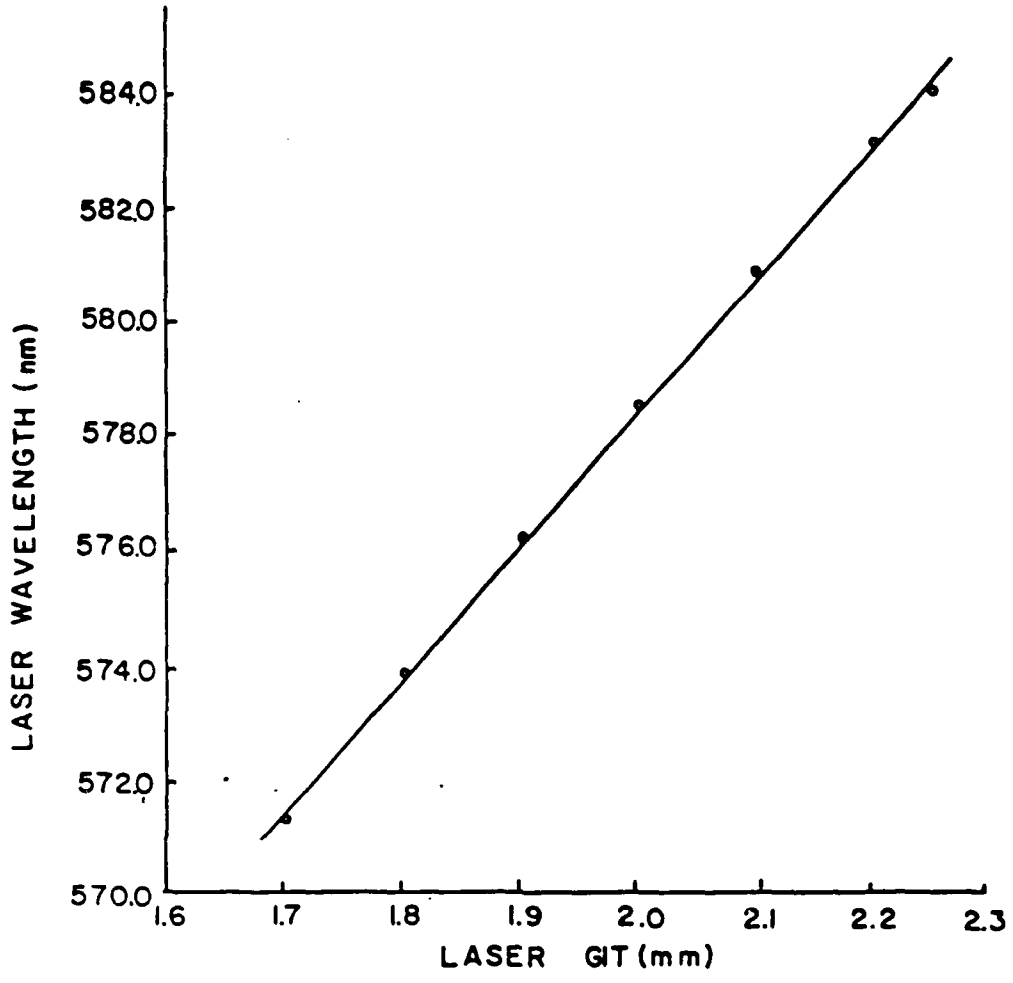

Figure 18. Dependence of wavelength of dye laser radiation on laser GIT setting.

The Fabry-Perot (FP) etalon was positioned to measure the dye laser output by removing one of the laser cavity mirrors and directing a HeNe beam along the same optical path as the laser output beam. The FP calibration was made using the HeNe laser as follows. The HeNe beam was focused by a 5-cm focal length lens located 10 cm in front of the etalon as shown in Fig. 19. The ring pattern was recorded on Polaroid or on 35-mm film at various distances behind the etalon. A typical ring pattern is shown in Fig. 20. The ring diameters, D_n, are related to wavelength, λ, etalon spacing, t, and distance from the focus of the light to the film plane, Y_o, by the relationship

$$Y_o^2 = \frac{2t}{8\lambda} (D_n^2 - D_{n-1}^2) \tag{29}$$

This relationship was checked by plotting the quantity $(D_n^2 - D_{n-1}^2)^{1/2}$ as a function of the distance Y from the film plane to the focusing lens. The results are presented in Fig. 21. The slope of this straight line is proportional to $2/\lambda t$ and the horizontal intercept, b', is the distance from the lens to the focal point of the laser beam. A least squares fit to the data points indicates the intercept to be 2.6 - 4.9 cm which agrees well with the anticipated value of 5 cm corresponding to the focal length of the lens. The slope predicts an etalon spacing of 0.444 cm which corresponds to a free spectral range (1/2 t) of 1.15 $\pm$ 0.03 cm^{-1}.

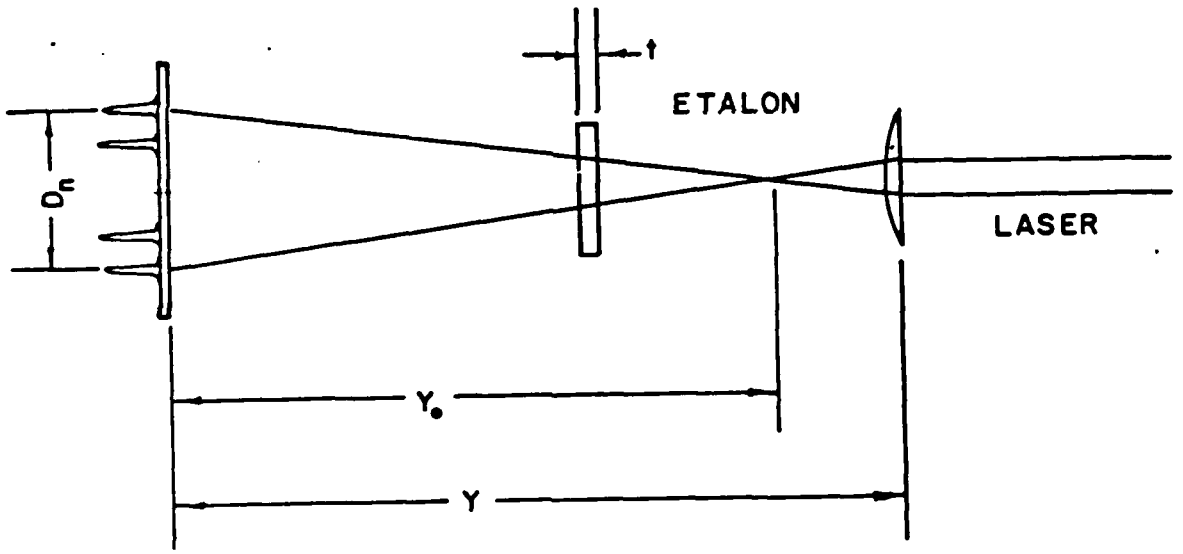

Figure 19. Geometry for Fabry-Perot interferometer.

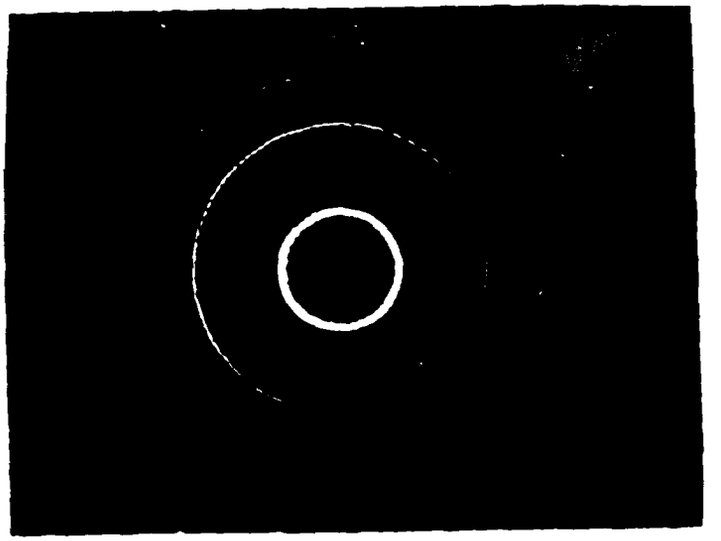

(a)

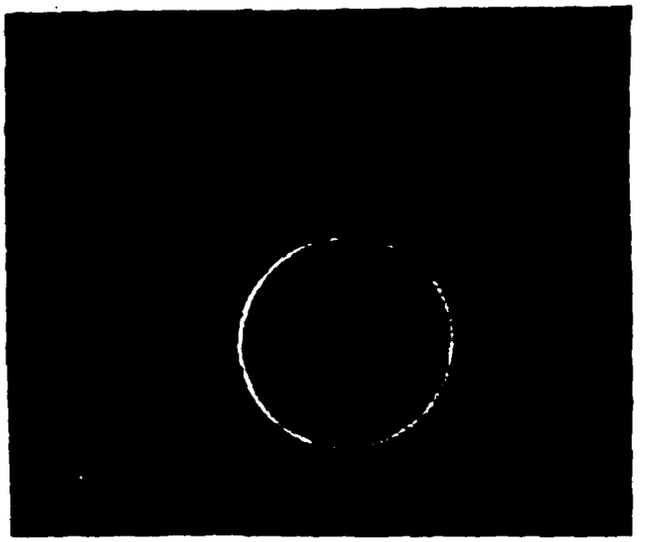

(b)

Figure 20. Fabry-Perot ring pattern of (a) HeNe laser and (b) dye laser.

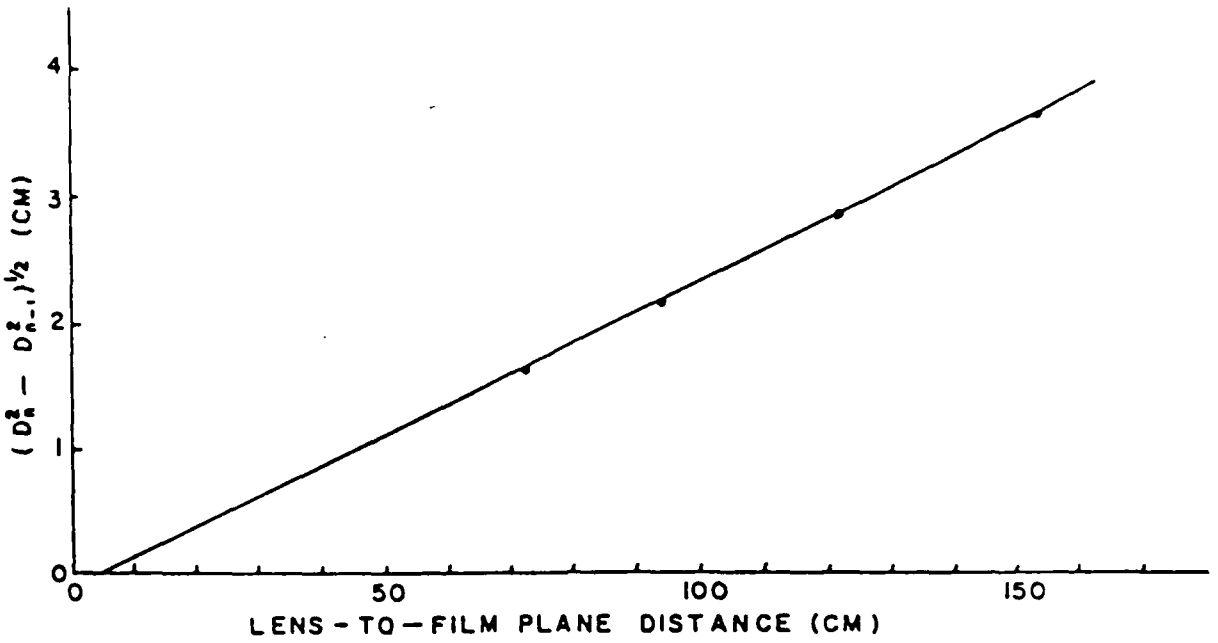

Figure 21. Relationship of average diameter of HeNe ring pattern obtained with Fabry-Perot interferometer on lens-to-film plane distance.

As a further check on this calibration and as an evaluation of the current analysis used to interpret the FP measurements, the FP patterns were recorded for a series of GIT settings. The GIT was varied by 0.001 mm increments so that a ring corresponding to a certain order in the interference pattern could be followed and identified. In this case, it is sufficient to measure the change in wavelength, $\Delta\lambda$, as the GIT setting is changed relative to some reference setting. The change in wavelength is related to the change in diameter of the nth order ring in the FP pattern by the relation

$$\Delta\lambda = \frac{\lambda^2}{2t}\left[\frac{D_n^2 - D_n^2(\text{ref})}{D_n^2 - D_{n-1}^2}\right] \tag{30}$$

where $D_n(\text{ref})$ is the diameter measured at the reference GIT setting (0.016 in this case) and D_n is the diameter of that same order ring at each value x

of the GIT setting. Since the change in wavelength should be linear with GIT setting x,

$$\Delta\lambda = mx \tag{31}$$

the quantity in parentheses in Eq. 30 is also linearly related to x

$$\left[\frac{D_n^2 - D_n^2(\text{ref})}{D_n^2 - D_{n-1}^2}\right] = \frac{2t}{\lambda^2} mx \tag{32}$$

This is shown in Fig. 22. The value of the free spectral range can be inferred from the slope of the curve in Fig. 22 if the value of 9.11 $\pm$ 0.5-nm/mm is used for the value of m. The value of 1.301 $\pm$ .045 cm^{-1} obtained in this fashion is 12 percent higher than the value obtained with the HeNe laser as described above. The agreement is sufficient to establish confidence in the F-P analysis that has been used to date to measure line widths. The error bars in Fig. 22 were obtained by calculating the difference in the squares of the outside and inside diameter of a given ring. These error bars represent the relative line widths of the individual measurements. Using the value of the free spectral range obtained above, the line widths are seen to vary from 0.0056 to 0.009 nm. Since these measurements are not made at the half-power points of the intensity pattern, the actual line widths are smaller than these values. Furthermore, the plotted points are observed to fluctuate around the average value by $\pm$ 0.0046 nm, which indicates the degree to which the laser frequency is known from the GIT setting. Measurements have been made under similar conditions where the laser line width is observed to vary and the central frequency is observed to fluctuate more than is indicated by the present results.

The laser line width is strongly influenced by the turbulence of the circulating dye in the flash lamp. The turbulence is determined by the temperature difference between the dye and cooling water temperatures, and the repetition rate of the laser. Experience has shown that frequency shifts from shot to shot can be minimized by waiting 1 min between shots to let the laser return to the equilibrium conditions.

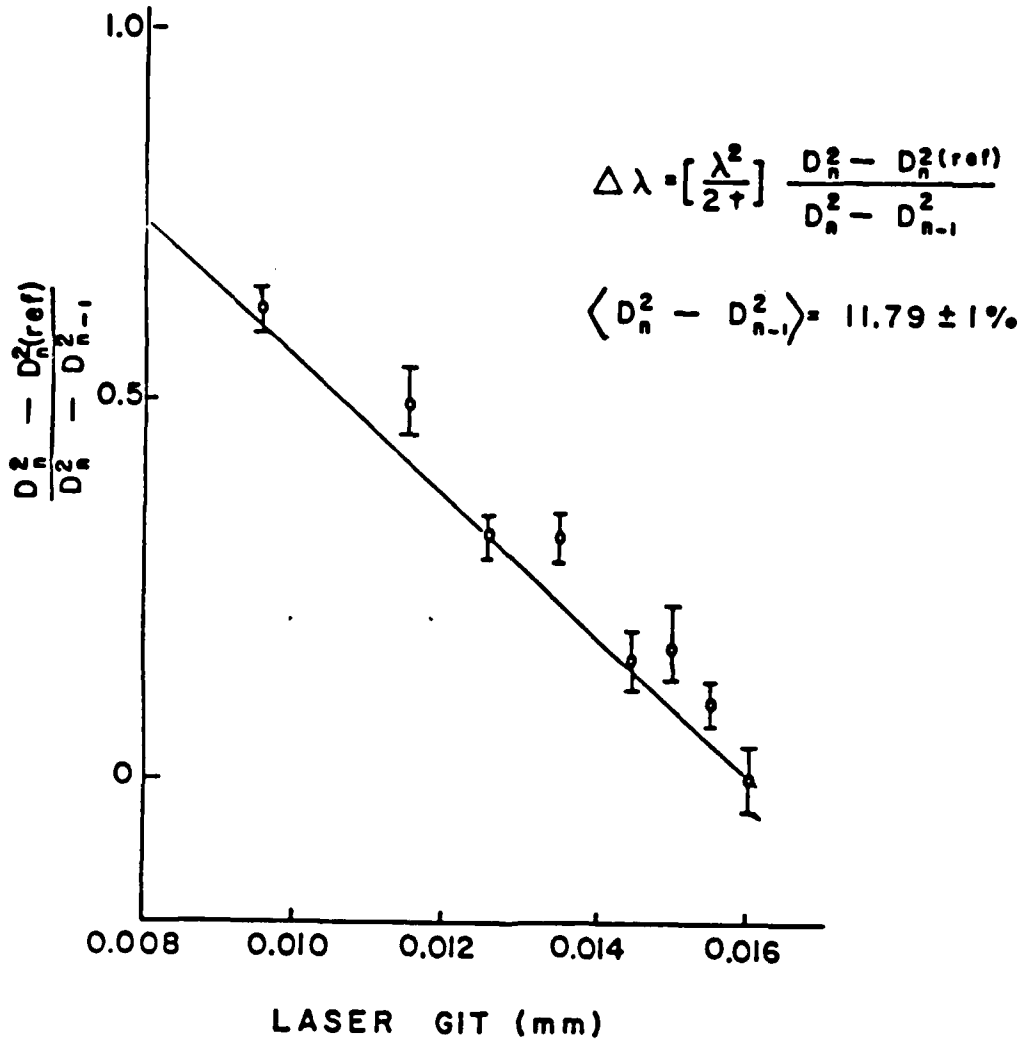

Figure 22. Linear dependence of laser wavelength on the micrometer setting of the GIT (0.009 nm/micron).

LASER INDUCED FLUORESCENCE

Laser-induced fluorescence was observed in neon discharges by tuning the laser to 585.25 nm. This was achieved by setting the monochrometer to the peak of the 585.25 line using a low pressure neon lamp and adjusting the GIT to find the line center. Figure 23 shows a typical laser line profile. The monochrometer measurements were normalized by measuring a fraction of the laser intensity using a diffusing collector and PIN diode arrangement. The diffusing collector consisted of a 0.65-cm-diam brass tube, with four diffusers 0.5 cm apart along the axis. This collector acted as an integrator to minimize variations in the monitor signal that were attributed to beam wander and not fluctuations in beam intensity. The observed line profile is indicative of the resolution limit of the monochrometer (0.02 nm) and not a measure of the laser line width.

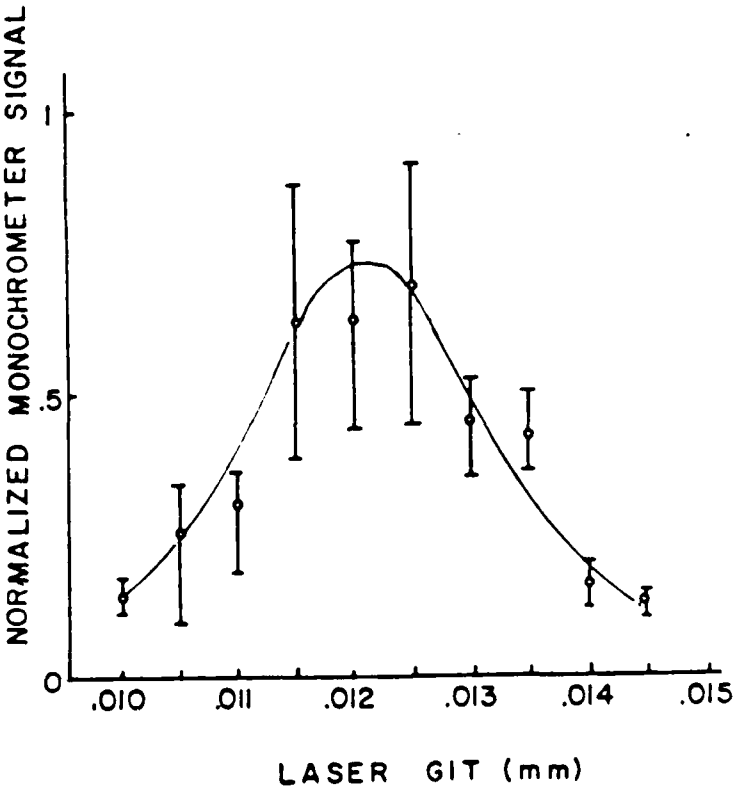

Figure 23. Laser line spectrum obtained with 0.02-nm resolution monochrometer.

LIF measurements were made on the 585.25-nm line of neon for currents in the range of 0.8 to 8 kA and for backfill pressures in the range of 67 to 1300 Pa. A typical photomultiplier signal showing a fluorescent radiation spike superimposed on the background emission signal is shown in Fig. 24 at the center of the discharge (a) and at an edge (b).

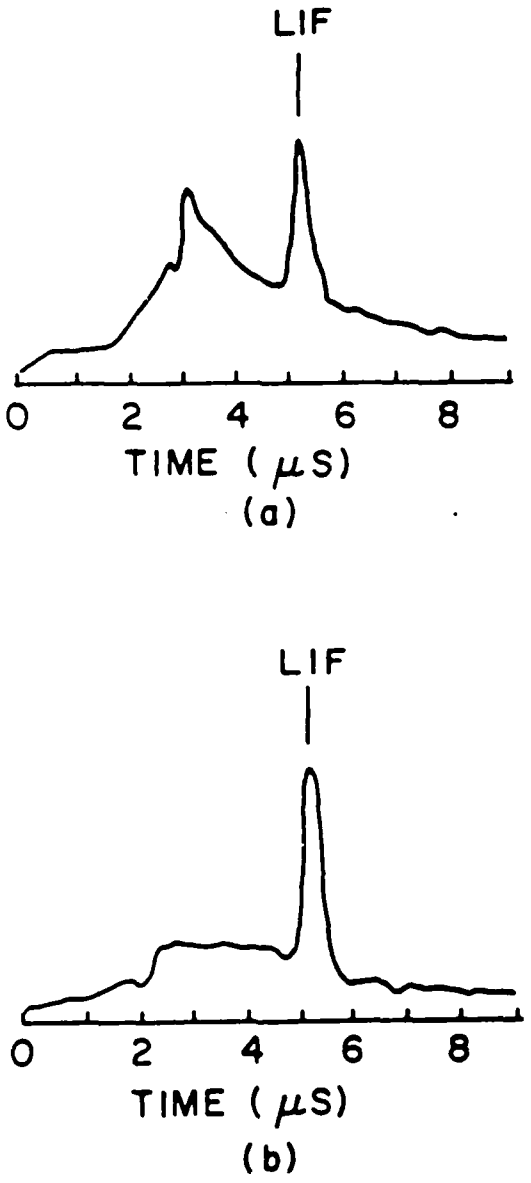

Figure 24. The total emission detected by a photomultiplier (a) at the center and (b) at the edge of the discharge, showing LIF emission spike superimposed on the background.

The dependence of the LIF intensity on laser power was measured and the results presented in Fig. 25. At low laser power levels, the LIF intensity increases linearly with power which saturates at high power levels. Most of the measurements presented here were made at the higher laser power levels. This reduced the requirement for normalizing all the measurements and minimized variations in LIF level due to fluctuations in laser power.

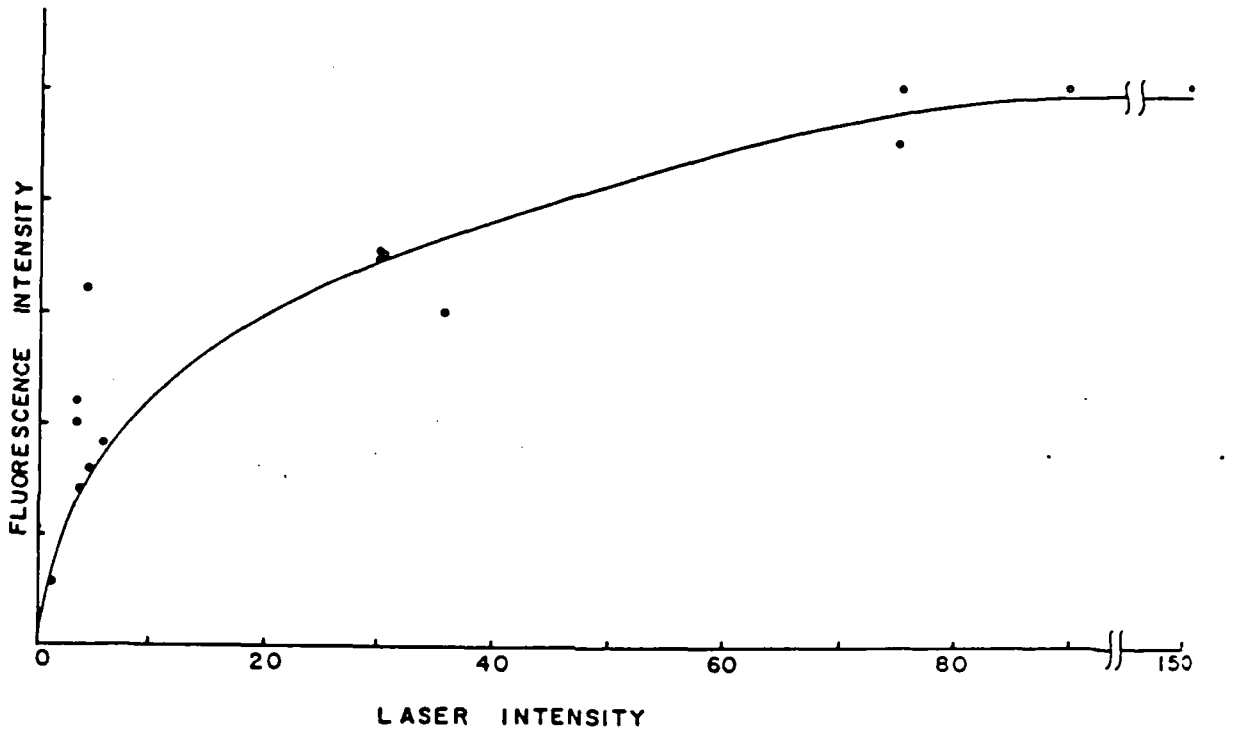

Figure 25. Dependence of LIF signal on laser intensity showing linear and saturated regimes.

The streak camera was not gated and therefore could not be used in these studies because the return sweep superimposed an image due to the afterglow plasma on the original streak image. This shortcoming imposed significant experimental complications on the project. Instead of measuring contours, it now became necessary to spatially resolve the LIF line profile by scanning the laser frequency for a series of transverse aperture positions. The following studies have been made.

The LIF spectrum was measured on the axis of the discharge tube at four different times in a 665-Pa neon discharge. The results are presented in Fig. 26. The plotted points are the average of three measurements and the error bars are the two extreme values observed. The peak current for these conditions was 1.3 kA. The laser wavelength, checked before and after the LIF spectrum measurements, was found to be centered at 0.0155 mm on the laser GIT control.

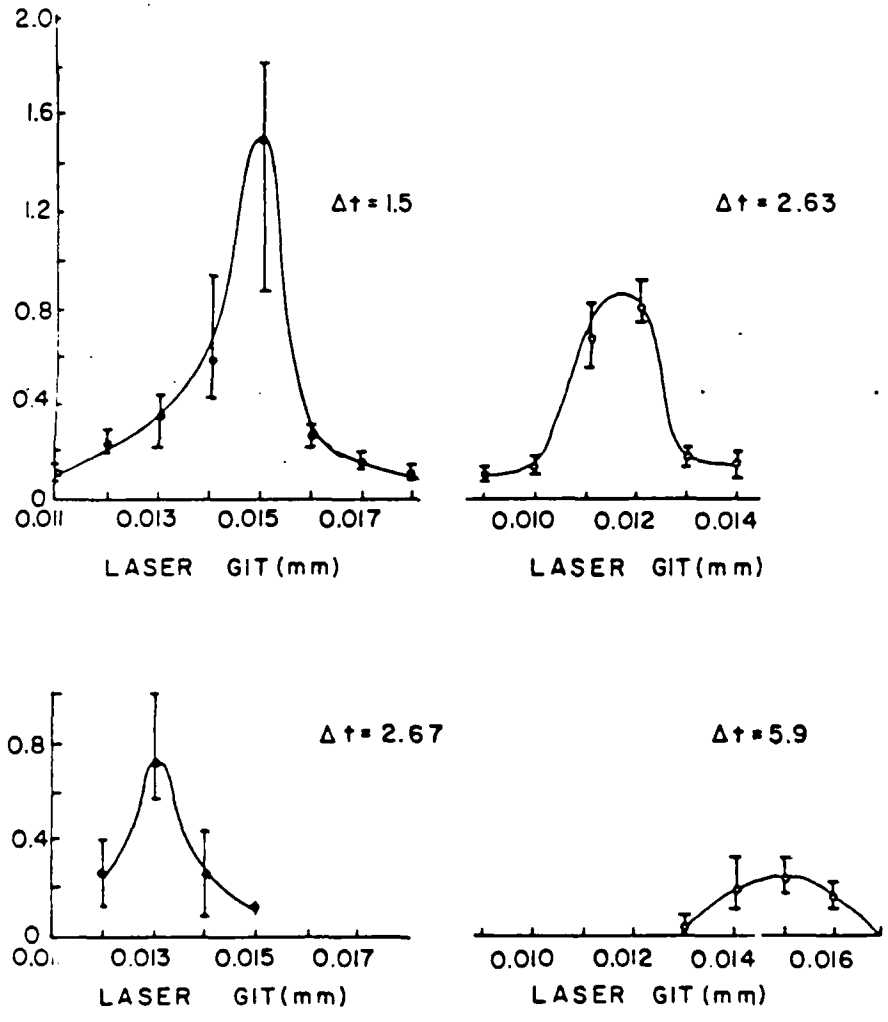

Figure 26. LIF spectra of 585.2-nm NeI in 665-Pa neon at various times (μs) after initiation of the discharge. Peak current is 1.3 kA and the wavelength change is 0.009 nm/micron.

The radial variation of the LIF spectrum was studied by measuring the line profile at the center of the column (a) and 0.57 cm from the center (b). The results are presented in Fig. 27 for conditions similar to those in Fig. 26. Note that the fluctuations are larger on the sides of the line, where small variations in laser wavelength can cause large changes in the LIF signal, than at the center of the line.

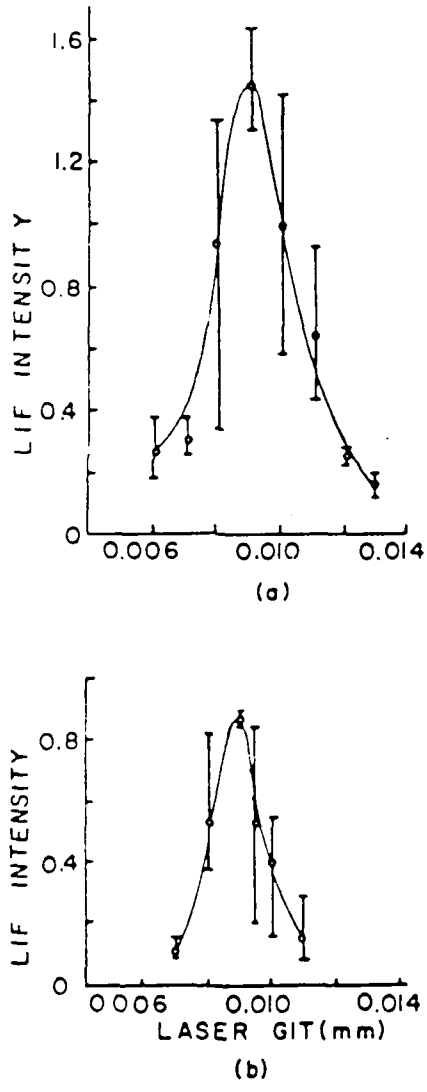

Figure 27. LIF spectrum of the 585.2-nm line in neon (a) on axis and (b) 0.6 cm from the centerline.

Measurements made at higher arc currents often exhibit a double-humped spectrum as shown in Figs. 28 and 29. The higher current spectra are invariably broader than the low current results shown in Figs. 26 and 27, although the symmetrical double-humped feature is not always as pronounced as in these measurements.

Measurements at larger arc currents were unsuccessful. The emission spectra of the 585.25-nm line indicated considerable broadening, which could account for the absence of any LIF signal. LIF was observed on the 585.25-nm NeI line for small additions of nitrogen (10 - 20%), but no LIF was observed in a 50/50 mixture.

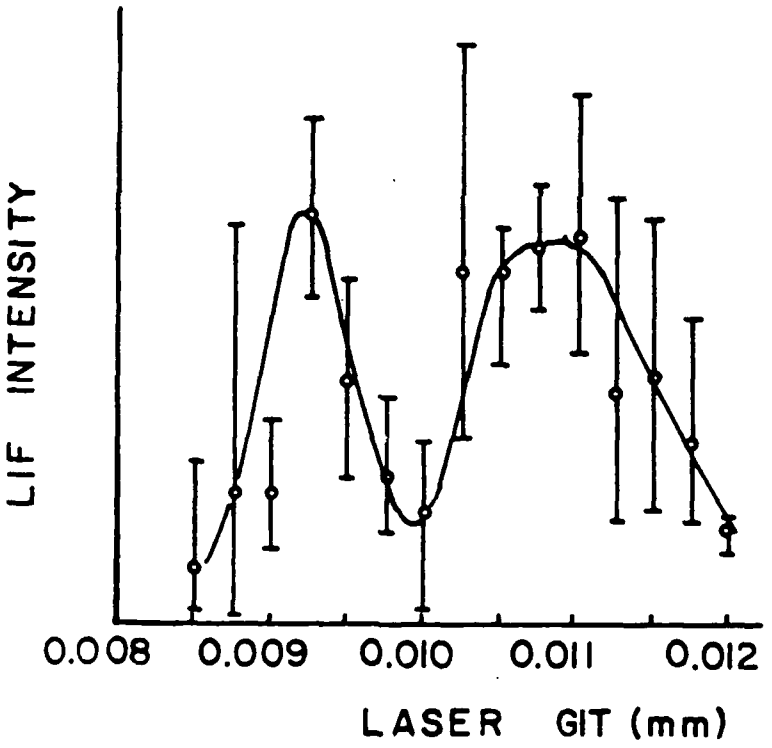

Figure 28. LIF spectrum of 585.2-nm NeI in a 3.6-kA discharge in neon at 532 Pa. (0.009 nm/ μm).

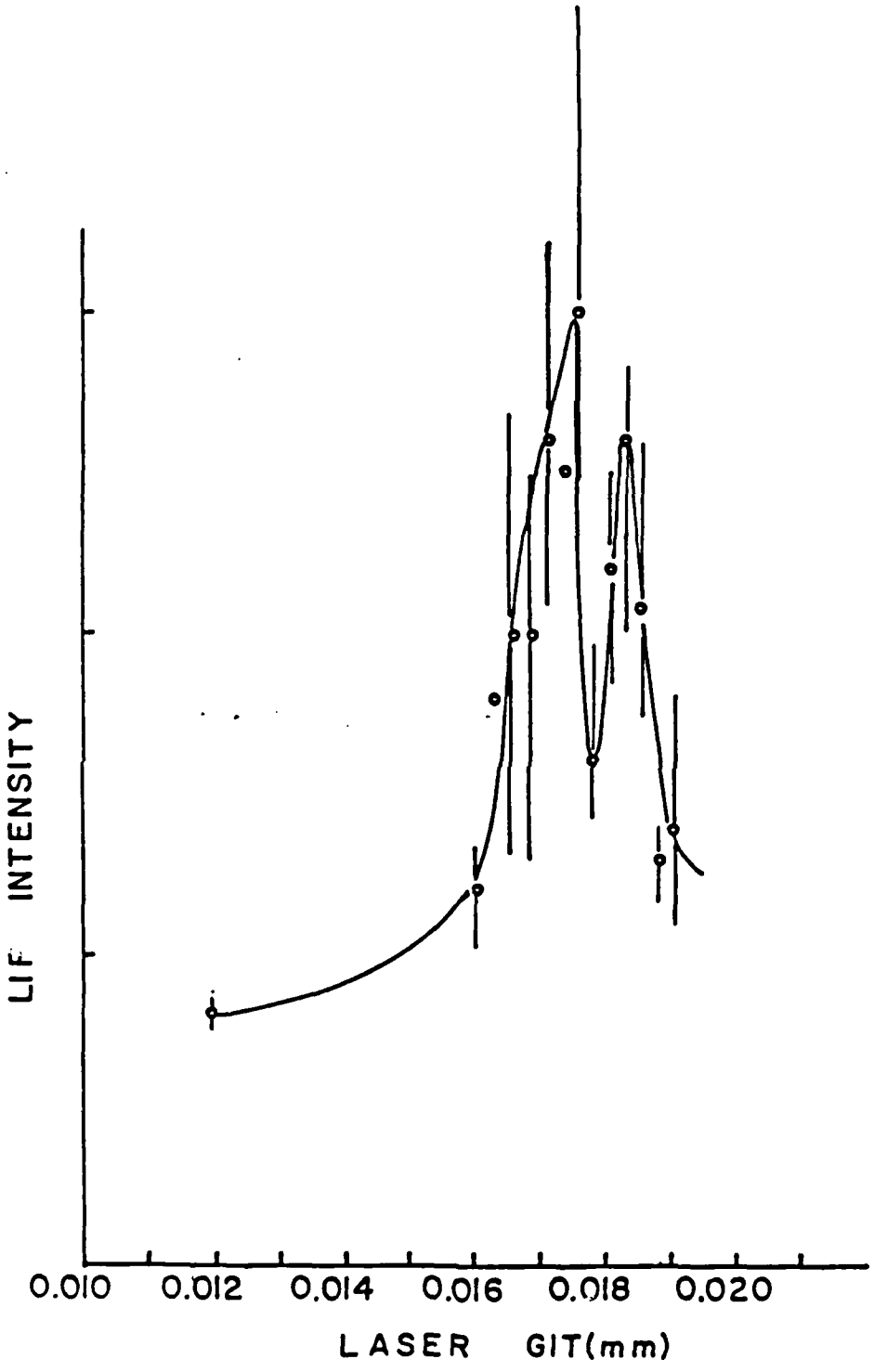

Figure 29. LIF spectrum of 585.2-nm NeI in a 2.9-kV discharge in neon at 532 Pa. (0.009 nm/μm).

LIF ON 566.664-nm N II LINE

A narrow band (0.08-nm) interference filter was obtained from Andover Corporation to study the 566.664-nm line of N II. The discharge was used as a source of 566.664-nm radiation to check the center frequency and band-pass of the filter. The transmission through the filter was measured as a function of the micrometer drive used to rotate the filter. The transmission values were normalized by the PIN diode signal used to monitor the discharge intensity and the results presented in Fig. 30. The relative magnitude and positions of the 566.66, 567.6 and 567.95-nm lines are also shown on the figure. The filter was tilted to the proper angle and the laser was tuned to the proper frequency using the monochrometer. For these latter measurements, the monochrometer was set to the peak of the 566.664-nm line using the discharge emission. The laser frequency was scanned through the center frequency for a range of nitrogen pressures (4 Pa to 13 kPa) and a range of discharge currents (0.8 - 20 kA) that spanned the range of parameters where LIF was observed on the 5852 line of NeI. In spite of repeated attempts to realign the system, vary the system parameters and carefully double-check the system calibration, no evidence was found for LIF on the 566.664-nm line of nitrogen.

ABSORPTION MEASUREMENTS

The laser radiation transmitted through the plasma was measured as the laser wavelength was scanned over the range of wavelengths where LIF was observed in neon. The laser intensity was attenuated to minimize the effect of saturating the transition, although no quantitative check was made. Figure 31 presents the average values (open circles) and error bars for the transmission measurements along with LIF measurements on the same discharge (crosses). The half micrometer shifts of the two peaks is of the order of magnitude variation in wavelength that was observed in the Fabry-Perot measurements (Fig. 22) and is not considered significant. The dip in the transmission can be used to estimate the absorption coefficient, K, which can be related to the density of absorbing atoms N* by the expression (Ref. 23)

$$K = \frac{N^* f H}{B} \qquad B = \frac{\omega V_{th}}{c} \tag{33}$$

Here f is the absorption oscillator strength, H is an integral over the Doppler shifted line profile and B is the Doppler shift of the line center frequency due to thermal motion of the absorbers (v_{th}). Using Measures' (Ref. 23) value for H and assuming room temperature neutrals, the concentration of absorbing neutrals is estimated to be $7 \times 10^{11}/cm^3$. If one further assumes, as before, that concentration can be attributed to an excitation temperature associated with the electron, a value of 1.25 eV is deduced for T_e.

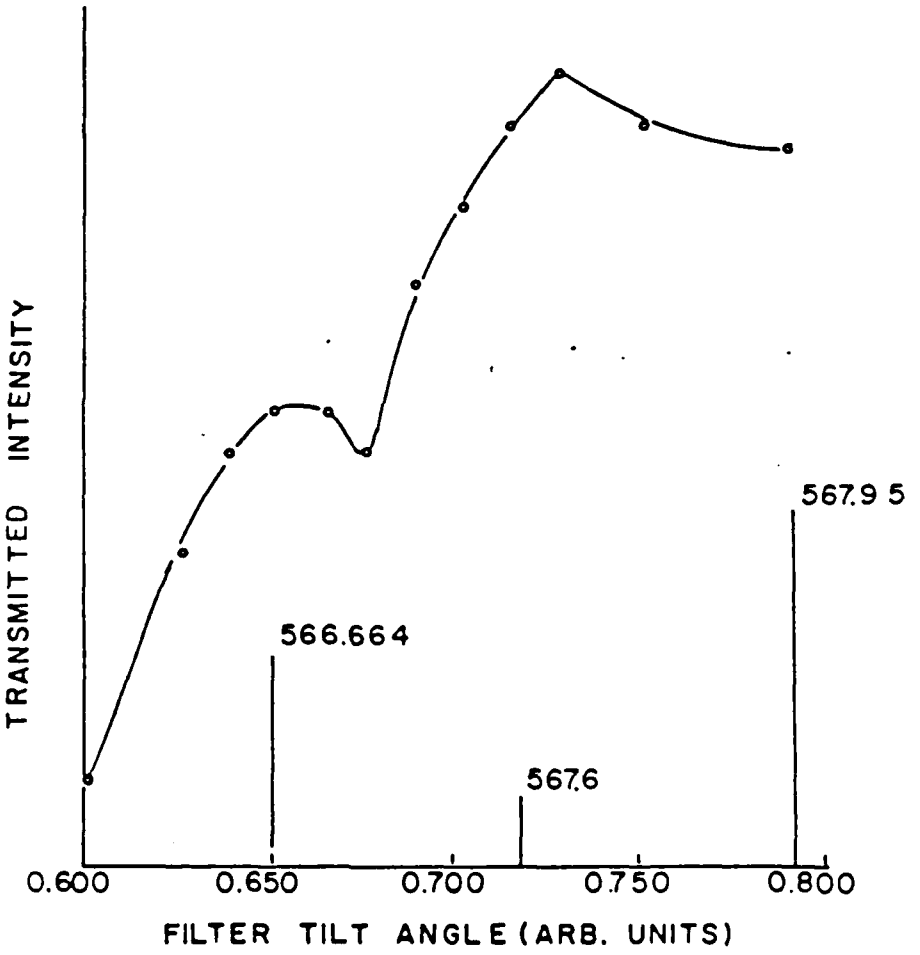

Figure 30. Transmission through interference filter as a function of micrometer setting tilting the filter. (Also shown are the relative magnitude and calculated positions of three N II lines in the pass band of the filter.)

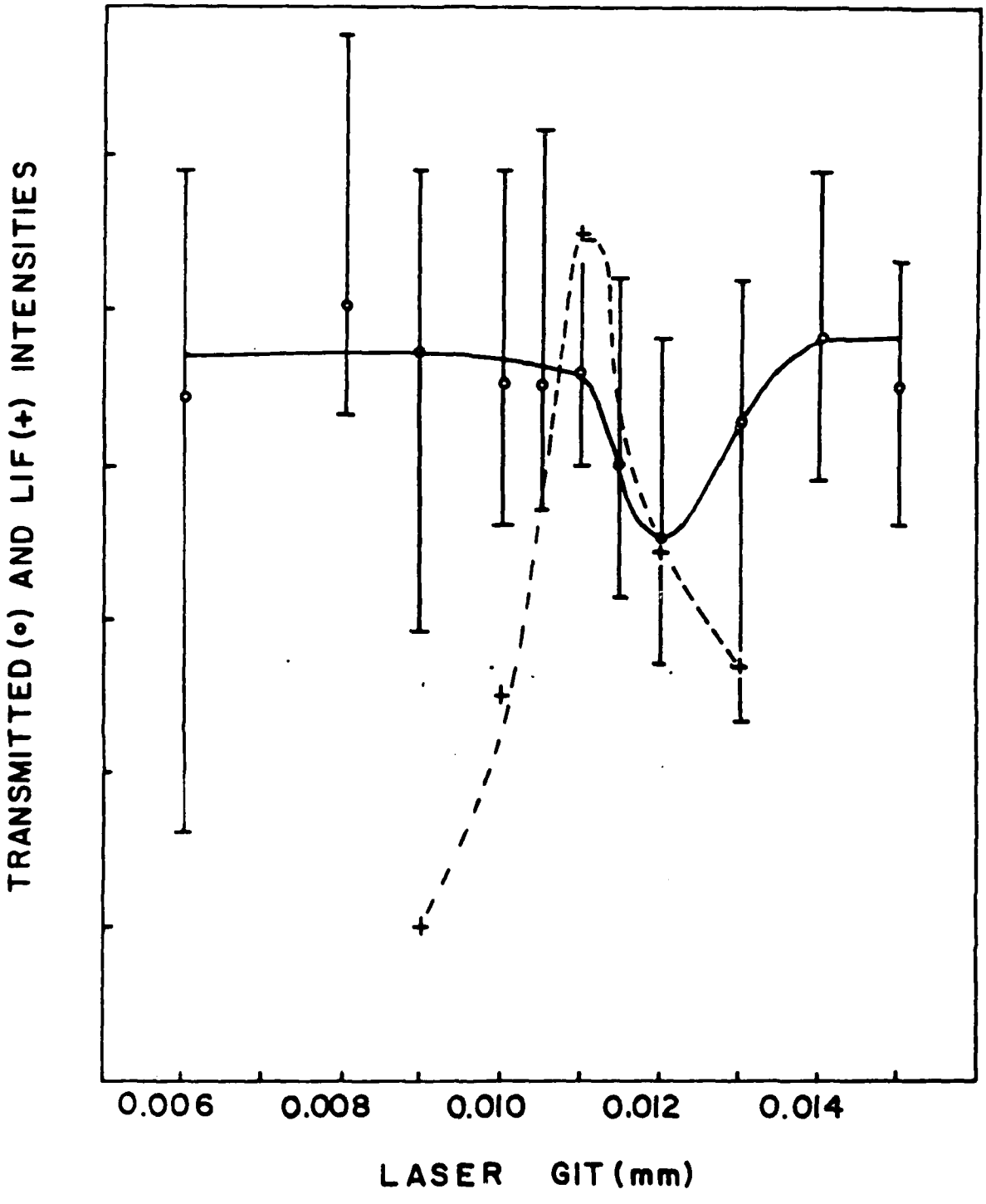

Figure 31. Laser transmission intensity (O) in 665-Pa neon discharge as the laser wavelength is tuned through 585.2-nm line. (The LIF intensity for similar conditions is shown by the crosses and dashed lines.)

V. DISCUSSION OF RESULTS AND SUGGESTIONS FOR FUTURE WORK

Laser induced fluorescence of the 585.25 NeI and 566.664-nm N II atomic transitions was studied in the arc discharge over a range of currents (0.8 to 30 kA) and pressures (40 Pa to 13 kPa). The LIF was observed only on the NeI line and only over a limited range of the parameter space probed. An understanding of these results requires an examination of the plasma conditions encountered in the discharge. Since the probe, emission, absorption and LIF measurements were not all made under the same condition, it is necessary to look for self-consistency in the results.

The Langmuir probe, absorption and LIF measurements were made at relatively low currents under similar conditions. The Langmuir probe values for the electron temperature (a few tenths of an eV) and the absorption measurement value (1.25 eV) have already been quoted. The electron temperature can also be inferred from the LIF measurements using the enhancement factor and Eq. 26. The values of Te obtained for the LIF spectra shown in Fig. 26 are presented in Table 4 assuming $V_P = V_{LIF}$ and $V_P/V_{LIF} = 2.87$ is given by the ratio of the plasma diameter to the laser beam diameter. The electron temperatures predicted by LIF measurements should still be considered upper limits, since broadening of the line due to magnetic field or Stark broadening effects will result in a reduced enhancement factor. In these cases, integrals over the line profile are required. The LIF measurements indicate that heating occurs during the discharge, as might be expected. The values obtained are somewhat larger than the Langmuir probe values and about the same as the absorption measurements near the peak of the current cycle (5.1 μs).

TABLE 4. ELECTRON TEMPERATURE (in eV) INFERRED FROM THE LIF SPECTRA AT VARIOUS TIMES IN THE DISCHARGE

T (μs)	$T_e(1)$	$T_e(2.87)$
1.51	1.24	0.82
2.63	1.14	0.78
2.67	1.78	1.1
5.9	2.21	1.32

The emission measurements at large currents (20 - 30 kA) indicate electron temperatures in the range of 2 to 3.5 eV, which are somewhat larger than the values obtained at lower current as described above. The only numbers with which these measurements can be compared are temperatures inferred from the expansion velocity observed for the plasma column as described in Section III. If the expansion velocity of 2×10^6 cm/s is equated to the ion sound speed, a value of 3 eV is inferred for the electron temperature which is consistent with the temperatures inferred from the line intensity ratios.

To determine whether the temperatures and densities inferred from these measurements are reasonable requires a consideration of the plasma conditions anticipated in arc discharges carrying currents of 0.8 to 36 kA. At the upper end, a pinched plasma column satisfying the Bennett Pinch condition and possibly local thermodynamic equilibrium is anticipated. The Bennett Pinch condition equates the magnetic pressure to the internal particle pressure (Ref. 24). For a 32-kA plasma column 1.71 cm in diameter, the electron density is predicted to be between 3.4 and $2 \times 10^{17}/cm^3$ for electron temperatures between 2 and 3.5 eV. These numbers compare very well with electron density of 3.7×10^{17} inferred from the Stark line width for the same arc current conditions. The Saha equilibrium relation predicts electron densities in the range of 1 to $2 \times 10^{17}/cm^3$ for the same range of temperatures (Ref. 25). These results taken as a whole indicate that a pinched arc is formed with electron densities a few times $10^{17}/cm^3$ and plasma temperatures of 2 - 3.5 eV for arc currents in the range of 30 kA.

If the Bennett Pinch relationship is applied to a 6 kA current in 530-Pa neon, the electron density is predicted to be 1 - 3 times $10^{16}/cm^3$ for electron temperatures in the range of 0.8 to 2 eV. Thermodynamic equilibrium predicts the following electron densities for each of the electron temperatures (Table 5). Also shown in Table 5 are the electron drift velocities which would be required for a 6-kA current in a 1.0-cm-diam arc. The electron drift velocities are expected to be less than the thermal velocity where plasma instabilities would be expected to heat the electrons and increase the ionization. This should occur for electron temperatures between 1.1 and 1.2 eV in Table 5. These temperatures are consistent with the temperatures inferred from the LIF measurements and the absorption measure-

ments. Furthermore, the electron densities in LTE are consistent with the Bennett relationship. The self consistency of these results indicates that the lower probe values are probably not indicative of the plasma conditions.

TABLE 5. ELECTRON DENSITIES CALCULATED FOR LTE CONDITIONS IN 530-Pa NEON AND ASSOCIATED DRIFT VELOCITIES FOR 6-kA BEAMS

Te	Ne(LTE)	v_d(cm/s)
0.5	1.82×10^{10}	9.5×10^{11}
0.7	1.13×10^{13}	1.52×10^{9}
0.9	4.3×10^{14}	1.2×10^{8}
1.1	4.53×10^{15}	1.1×10^{7}
1.2	4×10^{16}	1.3×10^{6}
1.4	8.77×10^{16}	1.9×10^{5}

The LIF line profiles obtained at 1.3 kA (Fig. 26) are Lorentzian line shapes that are definitely different from the double-humped profiles obtained at 3.6 kA (Fig. 28). Since this double-humped distribution occurs on many occasions, it cannot be dismissed as an experimental artifact without additional study. However, possible physical explanations for its characteristics can be made. First, the temperature measurements indicate that the radiation absorption length in 530-Pa neon, at an excitation temperature of 1.25 eV, is 51 cm. Under these conditions, the double-humped nature cannot be attributed to self-absorption. The widths of the LIF lines in Figs. 26 and 28 can be used together with Eq. 4 for the Stark width to infer the electron densities. The values obtained in the 1.3- and 3.6-kA arc discharge are 3×10^{16} and 8×10^{16} respectively. These values can be compared with the anticipated values obtained from a Bennett Pinch analysis. If the electron and ion temperature is assumed to be 1.25 eV, and the plasma radius is assumed to be 1 cm (the radius of the emitting region in Fig. 14), then

the electron densities are estimated to be 0.85 and 6.5 x 10^{16}/cm for the 1.3- and 3.6-kA cases. These predicted values are of the same order of magnitude as those inferred from the width of line, and the line broadening could be due entirely to Stark broadening. However, this effect cannot explain the double-humped feature. A possible explanation is Zeeman splitting described below.

The magnetic field in a current carrying column increases from the center of the column to some edge, at which point it begins to decrease inversely with radius. The Zeeman splitting of the line would follow the magnetic field strength, and the line profile measured in such a system would normally be a convolution of the number density of radiators in a given field and the shift at that field strength. This would produce a line whose maximum width corresponds to the maximum field strength. In a high current arc, the number density of neutrals in the center, where the magnetic field strength is small, can be severely depleted. This would reduce the observed LIF intensity at the line center and most of the detected radiation would correspond to radiators outside the arc where the field is large, producing a double-humped line profile similar to that shown in Fig. 28. This picture of reduced neutral radiators in the arc interior is consistent with the emission profile shown in Fig. 14.

The peak-to-peak separation is taken to be twice the Zeeman shift which has been estimated to be 0.00165-nm/kg. A 4.2 kg field is required to produce the 0.007-nm splitting observed. Since the arc current was 3.6 kA when these measurements were made, the arc radius would have to be 0.17 cm to produce a peak field of this magnitude. Since no spatial profile measurements were made on the ionic emission from the arc, a definite arc radius is not known. However, the value of 0.17 cm is consistent with the observations of others (Ref. 26).

Although some LIF was observed at higher arc currents, the signal was too small and unreproducible to allow LIF spectra to be obtained. No LIF was observed on the very high arc currents (15 - 30 kA). This could be due to a number of factors. As the excitation temperature is increased from 0.8 eV to 2 eV, the enhancement given by Eq. 25 decreases from 4.35 to 1.4, making the signal harder to separate from the background. Furthermore, any additional Stark or Zeeman broadening would reduce the number of absorbers

in the pass band of the laser. A slightly broader band laser might have facilitated LIF enhancement measurements integrated over the line width to be made, and the evolution of the excitation temperature to be studied. However, emission line profiles of the 585.2-nm line have indicated a severely broadened line which could account for the lack of LIF observation at high currents.

The absence of any LIF observations at the 566.664-nm N II line is without explanation. Unsuccessful attempts were made in pure nitrogen and in nitrogen/neon mixtures where the LIF of the 5852 NeI line was observed. These studies were conducted over broad pressure and current ranges that encompassed the conditions where LIF on the neon line was observed. The interference filter might have been broad enough so that the stronger 567.9 N II line obscured the enhancement of the 566.7 line, but no explanation is presently available.

In summary, LIF of the 585.25 NeI line was observed in arc discharges for a range of arc currents (0.8 to 5 kA). The excitation temperatures inferred from these LIF measurements (0.8 - 1.5 eV) agree reasonably well with the temperatures inferred from absorption measurements (1.25 eV) and estimates of the electron temperature using LTE calculations or Bennett Pinch analysis. Furthermore, these temperature measurements are slightly less than the excitation temperatures (2 - 3 eV) inferred from line intensity ratio measurements at high arc currents. A double-humped LIF spectrum has been observed on many occasions. The width of the line and the separation between the peaks are larger than the laser line width and the frequency variation observed with a Fabry Perot interferometer. These features do not appear to be instrumental in nature. The electron densities inferred from the width of the line using Stark broadening analysis are consistent with the density predicted by the Bennett Pinch model. However, the double-humped feature cannot be attributed to self-absorption. The separation in the peaks is consistent with Zeeman splitting if the arc channel is 0.34 cm in diameter. This arc diameter is consistent with observations of others, especially at higher pressures, but has not been confirmed by any in-house measurements.

The LIF studies were carried out on the discharge plasma to demonstrate the feasibility of using this technique to measure magnetic fields of a

relativistic electron beam propagating in a gas. The discharge is a good simulation of beam propagation problems associated with Stark broadening because comparable electron densities can be generated. Reductions in signal strength, and "washing out" of contour lines due to this effect, will occur in the propagation situation and can be studied here. Unfortunately, the electron temperatures and hence excitation temperature in the discharge (1 - 2 eV) are larger than those encountered in propagation studies (0.49 - 0.56 eV). Since the temperature appears in the exponent of the enhancement factor, small differences in the excitation temperature result in large differences in the amplitude of the LIF signal. An LIF signal which would be 9 times the background level in the propagation study would only be 0.4 times the background in a discharge. In this regard, the present studies are not a good simulation of what might be achievable in a beam study.

FUTURE WORK

The work to date suggests that Zeeman splitting of the 585.2-nm NeI line might have been measured by LIF spectroscopy in a pulsed discharge. The important ramification of this interpretation of the data to the beam propagation program suggests additional work is in order to confirm or deny this assertion. The magnetic field should be determined by measuring the current channel diameter using Langmuir probes, or measuring the radial distribution of an ionic line and inferring the field from the known current. The more definitive experiment that should be carried out is to measure the spatial distribution of the LIF radiation in order to observe the magnetic field contour directly. This should be recorded in one event, using a streak or a framing camera, to avoid the problems associated with reproducibility of the arc discharge and stability of the laser system encountered in the LIF spectral measurements carried out in the present study. An etalon added to the laser cavity to reduce the laser line width would allow greater resolution in measurements made in lower field strength regions.

The LIF studies on the 566.664 nm N II line should be discontinued in favor of the 343.716 nm atomic nitrogen ion line. This line has a Zeeman spectrum which is simpler than the 566.66 nII line and a Stark width which is slightly less. The enhancement factor is substantially larger (351 compared to 10.1 for a 0.5 eV excitation temperature) which leads to better signal to noise characteristics and better spatial resolution.

REFERENCES

1. G. T. Razdobarin, V. V. Semenov, L. V. Sololova, I. P. Folomkin, V. S. Burakov, P. Ya Misakov, P. A. Naumenkov and S. V. Nechaev, "An Absolute Measurement of the Neutral Density Profile in the Tokomak Plasma by Resonance Fluorescence on the H Line," Nuclear Fusion 19, 1441 (1979).

2. R. A. Gottscho, R. H. Burton, D. L. Flamm, V. M. Donnelly, and F. P. Davis, "Ion Dynamics of rf Plasma Sheaths: A Time-Resolved Spectroscopic Study," J. Appl. Phys. 55, 2707 (1984).

3. P. G. Weber and R. M. Erickson, "Zeeman Splitting Magnetic Field Diagnostic," Bull. Am. Phys. Soc. (1981).

4. W. P. West, J. S. deGrassie, J. F. Baur and E. S. Ensburg, "Possibility of Observation of Magnetic and Density Fluctuations with a Current Density Profile Diagnostic System," Bull. Am. Phys. Soc. 26, (1981).

5. Y. Maron and C. Litivin, "Spectroscopic Doppler-Free Methods for Measuring the Electric and Magnetic Fields in Magnetically Insulated Ion Diodes," J. Appl. Phys. 54, 2086 (1983).

6. H. R. Griem, Spectral Line Broadening by Plasmas, Academic Press, New York 1974.

7. H. R. Griem, Plasma Spectroscopy, McGraw-Hill, New York (1964).

8. J. Kielkopf - private communications, University of Louisville, Louisville, Kentucky, 1984.

9. N. Konjevic and J. R. Roberts, "A Critical Review of the Stark Widths and Shifts of Spectral Lines From Non-Hydrogenic Atoms," J. Phys. Chem. Ref. Data 5, 209 (1976).

10. S. Ch'en and M. Takeo, "Broadening and Shift of Spectral Lines Due to the Presence of Foreign Gases," Rev. Mod. Phys. 29, 20 (1957).

11. N. Allard and J. Kielkopf, "The Effect of Neutral Nonresonant Collisions on Atomic Spectral Lines," Rev. Mod. Phys. 54, 1103 (1982).

12. N. I. Kaliteevskii, E. M. Kotlikov and M. P. Chaika, "Determination of Atomic Constants and Collision Cross-Sections by the Method of Level Crossing in Gas Lasers," Sov. J. Quant. Elec. 7, 1107 (1977).

13. M. A. Gubin, A. I. Popov and E. D. Protsenko, "Pressure Dependence of the Line Width of the $3S_2$ - $3P_4$ Transition of Neon," Optics and Spectroscopy 25, 421 (1968).

14. R. Lemke - private communication, Air Force Weapons Laboratory, Kirtland Air Force Base, New Mexico, 1985.

15. J. W. Daily, "Laser Induced Fluorescence as an Engineering Tool," Proc. Soc. of Photo-Optical Instrumentation Engineers, Unconventional Spectroscopy 82, 146 (1976).

16. A. Yokoyama, S. Takao, R. Ueno and Y. Hatano, "Measurements of Deexcitation Rate Constants of Ne ($^3P_2$, ^3P_o, and $^3P_1$) by N_2 and SF_6 Using a Pulse Radiolysis Method," Chem. Phys. 45, 439 (1980).

17. A. V. Phelps, private communication, Joint Institute for Laboratory Astrophysics, National Bureau of Standards and University of Colorado, Boulder, Colorado, 1984.

18. R. E. Miers, J. E. Gastineau, M. H. Phillips, L. W. Anderson, and Chun C. Lin, "Electron Excitation Cross-Sections for the $1s_2$ and $1s_4$ Levels in Ne," Phys. Rev. A25, 1185 (1982).

19. L. R. Peterson and J. E. Allen, Jr., "Electron Impact Cross-Sections for Argon," J. Chem. Phys. 56,6068 (1971).

20. R. Johnston, private communication, Science Application, Inc., Los Altos, California, 1985.

21. G. Davidson and R. O'Niel, "Optical Radiation from Nitrogen and Air at High Pressure Excited by Energetic Electrons," J. Chem. Phys. 41, 3946 (1965).

22. J. Sheffield, Plasma Scattering of Electromagnetic Radiation, Academic Press, New York (1975).

23. R. M. Measures, "Spectral Line Interferometry: A Proposed Means of Selectively Measuring the Change in Density of a Specific Atomic Population," Appl. Opt. 9, 737 (1970).

24. D. L. Book, "NRL Plasma Formulary," Plasma Physics Division, Naval Research Laboratory, Washington, D.C. (undated compilation of formulas).

25. H. Drawin and P. Felenbok, Data for Plasmas in Local Thermodynamic Equilibrium, Gauthier-Villous, Paris (1965).

26. H. Tholl, Z. Naturforsch, 25a, 420 (1970).

END

10-87

DTIC